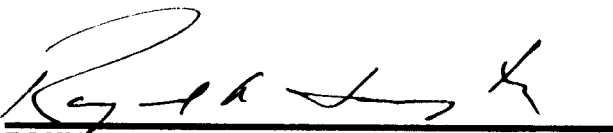


STATE OF CALIFORNIA
DEPARTMENT OF TRANSPORTATION
DIVISION OF FACILITIES CONSTRUCTION
OFFICE OF TRANSPORTATION LABORATORY

DEVELOPMENT OF WORST CASE
METEOROLOGY CRITERIA

Study Supervised byMas Hatano, P.E.
Principal InvestigatorPaul Benson, P.E.
Co-Principal InvestigatorWilliam Nokes, P.E.
AuthorsWilliam Nokes, P.E.
Paul Benson, P.E.
Project AssistantsDick Wood
Kenneth Pinkerman, P.E.
Jim Quittmeyer
Bob Cramer



RAYMOND A. FORSYTH, P.E.
Chief, Office of Transportation Laboratory

TECHNICAL REPORT STANDARD TITLE PAGE

1. REPORT NO. FHWA/CA/TL-85/14		2. GOVERNMENT ACCESSION NO.		3. RECIPIENT'S CATALOG NO.	
4. TITLE AND SUBTITLE Development of Worst Case Meteorology Criteria				5. REPORT DATE November 1985	
				6. PERFORMING ORGANIZATION CODE	
7. AUTHOR(S) W. A. Nokes and P. E. Benson				8. PERFORMING ORGANIZATION REPORT NO. 54328-604196	
9. PERFORMING ORGANIZATION NAME AND ADDRESS Office of Transportation Laboratory California Department of Transportation Sacramento, CA 95819				10. WORK UNIT NO.	
				11. CONTRACT OR GRANT NO. E80TL14	
12. SPONSORING AGENCY NAME AND ADDRESS California Department of Transportation Sacramento, California 95814				13. TYPE OF REPORT & PERIOD COVERED Final	
				14. SPONSORING AGENCY CODE	
15. SUPPLEMENTARY NOTES This study was conducted in cooperation with the U.S. Department of Transportation, Federal Highway Administration.					
16. ABSTRACT <p>A meteorological severity index (MSI) representing the relationship between meteorological parameters that contribute to worst case carbon monoxide concentrations near roadways is described. The MSI is based on sensitivity studies of the California Lines Source Dispersion Model, CALINE4. Meteorological data collected at several monitoring sites throughout California are described. Probabilistic analysis of the monitoring data (stratified by geography and time-of-day) is combined with the MSI to develop worst case meteorology inputs for estimating 1-hour CO levels using CALINE4.</p> <p>Worst case meteorology inputs are presented using peak and off-peak conditions for estimating worst case 8-hour CO levels when running the CALINE4 model. An alternative method of estimating worst case 8-hour CO levels is given by describing a "persistence factor". Guidelines are presented to help CALINE4 users develop or estimate an appropriate persistence factor for a project location.</p> <p>The probabilistic method described in the report can be used to establish new worst case meteorology criteria in the event of changes in the number of exceedances allowed by the National Ambient Air Quality Standards. The variety of locations studied in California should make results of the study useable by other states.</p>					
17. KEY WORDS Air pollution, highways, air quality, transportation, line source, dispersion model, meteorology, carbon monoxide, persistence factor.			18. DISTRIBUTION STATEMENT No restrictions. This document is available to the public through the National Technical Information Service, Springfield, VA 22161		
19. SECURITY CLASSIF. (OF THIS REPORT) Unclassified		20. SECURITY CLASSIF. (OF THIS PAGE) Unclassified		21. NO. OF PAGES	22. PRICE

NOTICE

The contents of this report reflect the views of the Office of Transportation Laboratory which is responsible for the facts and the accuracy of the data presented herein. The contents do not necessarily reflect the official views or policies of the State of California or the Federal Highway Administration. This report does not constitute a standard, specification, or regulation.

Neither the State of California nor the United States Government endorse products or manufacturers. Trade or manufacturers' names appear herein only because they are considered essential to the object of this document.

CONVERSION FACTORS

English to Metric System (SI) of Measurement

<u>Quality</u>	<u>English unit</u>	<u>Multiply by</u>	<u>To get metric equivalent</u>
Length	inches (in) or (")	25.40 .02540	millimetres (mm) metres (m)
	feet (ft) or (')	.3048	metres (m)
	miles (mi)	1.609	kilometres (km)
Area	square inches (in ²)	6.432 x 10 ⁻⁴	square metres (m ²)
	square feet (ft ²)	.09290	square metres (m ²)
	acres	.4047	hectares (ha)
Volume	gallons (gal)	3.785	litre (l)
	cubic feet (ft ³)	.02832	cubic metres (m ³)
	cubic yards (yd ³)	.7646	cubic metres (m ³)
Volume/Time (Flow)	cubic feet per second (ft ³ /s)	28.317	litres per second (l/s)
	gallons per minute (gal/min)	.06309	litres per second (l/s)
Mass	pounds (lb)	.4536	kilograms (kg)
Velocity	miles per hour (mph)	.4470	metres per second (m/s)
	feet per second (fps)	.3048	metres per second (m/s)
Acceleration	feet per second squared (ft/s ²)	.3048	metres per second squared (m/s ²)
	acceleration due to force of gravity (G) (ft/s ²)	9.807	metres per second squared (m/s ²)
Density	(lb/ft ³)	16.02	kilograms per cubic metre (kg/m ³)
Force	pounds (lbs)	4.448	newtons (N)
	(1000 lbs) kips	4448	newtons (N)
Thermal Energy	British thermal unit (BTU)	1055	joules (J)
Mechanical Energy	foot-pounds (ft-lb)	1.356	joules (J)
	foot-kips (ft-k)	1356	joules (J)
Bending Moment or Torque	inch-pounds (in-lbs)	.1130	newton-metres (Nm)
	foot-pounds (ft-lbs)	1.356	newton-metres (Nm)
Pressure	pounds per square inch (psi)	6895	pascals (Pa)
	pounds per square foot (psf)	47.88	pascals (Pa)
Stress Intensity	kips per square inch square root inch (ksi√in)	1.0988	mega pascals√metre (MPa√m)
	pounds per square inch square root inch (psi√in)	1.0988	kilo pascals√metre (KPa√m)
Plane Angle	degrees (°)	0.0175	radians (rad)
Temperature	degrees fahrenheit (F)	$\frac{+F - 32}{1.8} = +C$	degrees celsius (°C)

ACKNOWLEDGEMENTS

The authors appreciate the technical support provided by Mr. Ken Robertson during the field monitoring phase of the project and Ms. Susan Zygowicz during the data reduction phase. Special thanks go to Marti Corralejo, Joanne Gray, and Lydia Burgin who assisted and helped guide the preparation of this final report.

TABLE OF CONTENTS

	<u>PAGE</u>
LIST OF TABLES	iv
LIST OF FIGURES	vi
1. INTRODUCTION	1
2. BACKGROUND	2
3. CONCLUSIONS AND RECOMMENDATIONS	4
4. IMPLEMENTATION	8
5. DESCRIPTION OF MONITORING SITES & METEOROLOGICAL DATA	9
6. DEVELOPMENT OF A METEOROLOGICAL SEVERITY INDEX . .	15
7. DETERMINING WORST CASE METEOROLOGICAL SCENARIOS FOR MAXIMUM 1-HOUR AVERAGED CO CONCENTRATIONS	19
A. Introduction	19
B. Probabilistic Analysis	20
C. Curve-Fitting Using A Lognormal Function	32
D. Testing Goodness-of-Fit	36
E. Worst Case Wind Speed and Sigma Theta	36
F. Worst Case Stability Class and Temperature . . .	39
1). Stability Class	39
2). Temperature	40
G. 1-Hour Worst Case Meteorology	46
8. PREDICTING WORST CASE 8-HOUR CO CONCENTRATIONS . .	48
A. Introduction	48
B. 8-Hour Persistence Factor	50
C. 8-Hour Worst Case Meteorology	67
REFERENCES	77

LIST OF TABLES

	<u>Page</u>
3-1. Suggested Worst Case 1-Hour Meteorological Scenarios	5
3-2. Crosswind Case -- Suggested Worst Case 8-Hour Meteorological Scenarios	6
3-3. Parallel Case -- Suggested Worst Case 8-Hour Meteorological Scenarios	7
5-1. Monitoring Sites and Periods	10
6-1. CALINE4 Inputs for MSI Development	16
7-1. Probability, P_2 , for Time-of-day Periods	30
7-2. Correlation Coefficients Relating Wind Speed and Sigma Theta Dependence	33
7-3. Chi-Squared Statistic Test Results	37
7-4. National Weather Service and AQDHS Sites	41
7-5. January Mean Minimum Temperatures Showing Minimums for Three Years in Parentheses, OF	44
7-6. Suggested Worst 1-Hour Meteorological Scenarios	47
8-1. California Ambient CO Data Set	51
8-2. Statistical Characteristics of Persistence Factors in the California Data Set	54
8-3. Number of Stations in Each Air Basin in the CARB Ambient CO Network	61
8-4. Statistical Characteristics of Persistence Factors in Each Air Basin	63
8-5. Comparison of CDS Mean Versus CARB 3-Year Maximum Persistence Factors	68
8-6. Crosswind Case (Sigma Theta ≤ 45 degrees) Peak & Off-Peak Monitoring Data Summaries	73

LIST OF TABLES (Continued)

	<u>Page</u>
8-7. Parallel Case (Sigma Theta ≤ 15 degrees) Peak & Off-Peak Monitoring Data Summaries	74
8-8. Crosswind Case -- Suggested Worst Case 8-Hour Meteorological Scenarios	75
8-9. Parallel Case -- Suggested Worst Case 8-Hour Meteorological Scenarios	76

LIST OF FIGURES

	<u>Page</u>
5-1. Meteorological Monitoring Sites for Developing Worst Case Meteorology Criteria	11
5-2. Typical Trailer Mounted Meteorological Tower	12
7-1. (a) Wind Speed & Sigma Theta Histograms: Mammoth, Nocturnal Period	21
(b) Wind Speed & Sigma Theta Histograms: Half Moon, Nocturnal Period	22
7-2. (a) Wind Speed & Sigma Theta Histograms: Mammoth, Midday Period	23
(b) Wind Speed & Sigma Theta Histograms: Half Moon, Midday Period	24
7-3. Joint Probability Distribution of Sigma Theta with Wind Speed at Mammoth During (a) Nocturnal and (b) Midday Periods	26
7-4. Joint Probability Distribution of Sigma Theta with Wind Speed at Half Moon During (a) Nocturnal and (b) Midday Periods	27
7-5. Surface Described by the Joint Probability Density Function (PDF) in Equation 7-3	31
7-6. Surfaces Described by BLN PDF & MSI Functions	38
7-7. January Mean Minimum Temperatures Versus High-MSI Temperatures	43
7-8. Predicted Temperatures Using Adjustment Factor Versus High-MSI Temperatures	45
8-1. Ranges of Persistence Factors from CDS Sites.	53
8-2. Persistence Factors at Less Populated (<100 ^k) CDS Locations	55
8-3. Persistence Factors at Medium Populated (100 ^k -500 ^k) CDS Locations	56
8-4. Persistence Factors at Densely Populated (>500 ^k) CDS Locations	57

LIST OF FIGURES (Continued)

	<u>Page</u>
8-5 Cumulative Frequency Distributions of Persistence Factors	59
8-6. Ranges of Persistence Factors from CARB Summaries, 1981-83	62
8-7. (a) Cumulative Frequency Distributions of Persistence Factors in Coastal Basins (CARB data)	64
(b) Cumulative Frequency Distributions of Persistence Factors in Inland Basins (CARB data)	65
8-8. Maximum Persistence Factors from 1981-83 Versus Means from CDS	69

1. INTRODUCTION

The California line source computer model, CALINE4, published recently by the California Department of Transportation (Caltrans)(1), predicts concentrations of carbon monoxide (CO) and other vehicle-related air pollutants near transportation projects. CALINE4 is an updated and expanded version of the 1979 CALINE3 model(2). Both of these models attempt to relate meteorological parameters such as wind speed and atmospheric stability to the transport and dispersion of vehicle emissions. Selection of values for these parameters has a direct and significant effect on the predictions made by the models.

This report contains recommended worst case meteorological inputs for use with CALINE4. Recommended values for wind speed and directional variability, atmospheric stability, and temperature are described as a function of geography and land use. These recommended values are based on a statistical analysis of actual measurements made at a variety of locations in California.

The contents of this report are specifically tailored to applications of CALINE4 for microscale CO analyses. The influence of meteorology on air quality near roadways was assessed using a meteorological severity index (MSI) developed directly from CALINE4 output. The authors believe that the results will be useable by other states because of the variety of locations studied in California.

2. BACKGROUND

Federal law mandates that the environmental impact of proposed transportation projects be considered as part of the planning and design process. Air quality studies are often part of the impact assessment procedure. One aspect of these studies is to determine the "worst case" meteorology at proposed project sites. This is defined as a set of values for wind speed, wind direction, directional variability, atmospheric stability, and temperature which will yield the highest pollutant levels within a specific study area when combined with corresponding peak traffic emissions.

It is important to correctly characterize site-specific worst case meteorology so that maximum air pollution concentrations are accurately predicted for comparison to the National Ambient Air Quality Standards (NAAQS). In the absence of nearby, representative National Weather Service or airport weather stations, field measurements can be made at the site to accomplish this. However, collection and analysis of field measurements are the most expensive and time consuming aspects of air quality studies. Another method is to assume an absolute worst case scenario. This precludes the need for field meteorology measurements and guarantees a conservative estimate of air quality impacts. However, results can be unrealistic, particularly for 8-hour averages, because inherent variability in meteorology are often not accounted for in worst case methods.

A review of Caltrans air quality reports submitted throughout the 1970's indicated that field measurements of meteorology were often made hurriedly, if at all, and that the results were rarely applied in the dispersion modeling

process. Instead, an absolute worst case scenario evolved. A wind speed of 2 mph and the most stable atmospheric stability class (F) were usually assumed. In urban areas, neutral stability (D) was assumed because of the urban heat island effect. Wind direction was assumed parallel to the roadway and unvarying over eight hours. Use of absolute worst case meteorology was particularly prevalent on smaller projects whose planning and design budgets could not support costly data collection programs. It was often applied without regard for site characteristics, traffic distribution or wind direction persistence.

This report introduces a set of worst case meteorological scenarios based on representative field measurements for a variety of locations. Detailed micrometeorological measurements were made in typical mountain, valley and coastal areas of California. Where applicable, both rural and urban environments were investigated.

Morning, midday, evening and nocturnal worst case scenarios were developed for each combination of terrain and land use. Guidelines were prepared so that project engineers or planners could refer to the results of this research and use them as a guide for selecting worst case conditions when field investigations were not feasible.

3. CONCLUSIONS AND RECOMMENDATIONS

Meteorology data from several diverse locations throughout California are described after stratification by geography, land use, and time-of-day periods. Probabilistic characterization of these data is combined with the meteorological severity index (MSI) to develop worst case meteorology criteria for estimating 1-hour CO levels shown in Table 3-1. A lack of consistent difference between urban and rural data resulted in criteria that distinguish between geographic categories and time-of-day periods only.

Eight-hour worst case criteria are given for peak and off-peak conditions as shown in Table 3-2 and 3-3. Computing a locally derived persistence factor is presented as an alternative to the 8-hour worst case criteria. Default values are recommended for 8-hour persistence factors for rural, urban, and stagnant urban conditions since persistence factor values are found to correlate directly to land use.

Use of these results substantially reduces the need for monitoring meteorology conditions at project sites, thereby reducing project costs. This report provides inputs necessary for CALINE4 to estimate worst case air quality impacts. Therefore, it is recommended that these criteria be used with CALINE4 when estimating worst case pollutant levels.

Table 3-1. Suggested Worst Case 1-Hour Meteorological Scenarios.

Geographic Location	Wind Speed	Sigma Theta	Stab. Class	Δ Temp.
MORNING				
(0600-1000)				
Coastal	0.5	10	"G"	+5
Coastal Val.	0.5	20	"G"	+5
Central Val.	0.5	5	"G"	+5
Mountain	0.5	30	"G"	+5
MIDDAY				
(1000-1700)				
Coastal	1.0	25	"D"	+10
Coastal Val.	0.6	30	"D"	+10
Central Val.	0.5	20	"D"	+10
Mountain	0.9	30	"D"	+10
EVENING				
(1700-2100)				
Coastal	0.5	10	"G"	+5
Coastal Val.	0.5	10	"G"	+5
Central Val.	0.5	5	"G"	+5
Mountain	0.5	30	"G"	+5
NOCTURNAL				
(2100-0600)				
Coastal	0.5	5	"G"	0
Coastal Val.	0.5	15	"G"	0
Central Val.	0.5	10	"G"	0
Mountain	0.5	20	"G"	0

Note: Wind speed is in m/s, sigma theta in degrees, and Δ temperature in degrees Fahrenheit. Add Δ temperature to lowest January mean minimum temperature over three year period.

Table 3-2. Crosswind Case -- Suggested Worst Case
8-Hour Meteorological Scenarios.

Geographic Location	PEAK				OFF-PEAK			
	Wind Speed	Sigma Theta	Stab. Class	Temp.	Wind Speed	Sigma Theta	Stab. Class	Δ Temp.
MORNING								
Coastal	0.5	45	"G"	+5	1.5	30	"D"	+10
Coastal Val.	0.5	45	"G"	+5	1.0	45	"D"	+10
Central Val.	0.5	45	"G"	+5	0.5	45	"D"	+10
Mountain	0.5	45	"G"	+5	1.5	30	"D"	+10
MIDDAY								
Coastal	0.5	45	"G"	+5	1.5	30	"D"	+10
Coastal Val.	0.5	45	"G"	+5	1.0	45	"D"	+10
Central Val.	0.5	45	"G"	+5	0.5	45	"D"	+10
Mountain	0.5	45	"G"	+5	1.5	30	"D"	+10
EVENING								
Coastal	0.5	45	"G"	+5	0.5	45	"D"	+5
Coastal Val.	0.5	45	"G"	+5	0.5	45	"D"	+5
Central Val.	0.5	45	"G"	+5	0.5	45	"D"	+5
Mountain	0.5	45	"G"	+5	0.5	45	"D"	+5

Note: Wind speed is in m/s, sigma theta in degrees, and Δ temperature in degrees Fahrenheit.
Add Δ temperature to lowest January mean minimum temperature over three year period.

Table 3-3. Parallel Case -- Suggested Worst Case
8-Hour Meteorological Scenarios.

Geographic Location	PEAK				OFF-PEAK			
	Wind Speed	Sigma Theta	Stab. Class	Temp.	Wind Speed	Sigma Theta	Stab. Class	Δ Temp.
MORNING								
Coastal	1.0	20	"G"	+5	2.0	20	"D"	+10
Coastal Val.	1.0	20	"G"	+5	2.0	20	"D"	+10
Central Val.	0.5	20	"G"	+5	1.0	20	"D"	+10
Mountain	1.0	20	"G"	+5	2.0	20	"D"	+10
MIDDAY								
Coastal	1.0	20	"G"	+5	2.0	30	"D"	+10
Coastal Val.	1.0	20	"G"	+5	2.0	45	"D"	+10
Central Val.	1.0	20	"G"	+5	1.0	45	"D"	+10
Mountain	1.0	20	"G"	+5	2.0	30	"D"	+10
EVENING								
Coastal	1.0	20	"G"	+5	1.0	20	"G"	+5
Coastal Val.	1.0	20	"G"	+5	1.0	20	"G"	+5
Central Val.	1.0	20	"G"	+5	1.0	20	"G"	+5
Mountain	1.0	20	"G"	+5	1.0	20	"G"	+5

Note: Wind speed is in m/s, sigma theta in degrees, and Δ temperature in degrees Fahrenheit.
Add Δ temperature to lowest January mean minimum temperature over three year period.

4. IMPLEMENTATION

1. The worst case meteorology criteria recommended in this report will be provided to users of the CALINE4 program.

2. An air quality training course covering worst case meteorology criteria, use of the CALINE4 computer program, and other new assessment procedures will be conducted for state personnel.

5. DESCRIPTION OF MONITORING SITES & METEOROLOGICAL DATA

As part of this study, a series of comprehensive meteorological measurements were made at several sites representing a cross section of possible project locations within California. The major geographic classifications studied were coastal, coastal valley, central valley, and mountain. Site selection was based on adequate exposure, serviceability, and representativeness of the geographic and land use conditions for each classification. Where possible, sites were chosen in both urban and rural land use settings. Data from previous studies also were used to supplement the field measurements.

Table 5-1 summarizes the location and monitoring periods for the data base. The area and site codes refer to storage locations within the Caltrans Air Quality Data Handling System (AQDHS). Figure 5-1 shows locations monitored previously and stations established for this research. Sites monitored before 1980 were not established as part of this study, but contained useable measurements.

Figure 5-2 shows a typical meteorological tower. Wind speed, wind direction, and temperature were recorded at 10 m and 18 m above ground level. Sites were chosen in open areas so that the sensors had a clear fetch in all directions for at least 25 m. The only exception to this was the Mammoth Lakes site, located in a grove of scattered, 15 m high pine trees. The meteorological towers and automated data acquisition systems are described in detail in an earlier Caltrans report(3).

Table 5-1. Monitoring Sites and Periods.

GEOGRAPHY/LAND USE LOCATION	AREA CODE	SITE CODE	MONITORING PERIOD
COAST--URBAN Convair	6820	001	10/9/75-12/7/75
COAST--RURAL Half Moon Bay	3090	101	1/9/81-4/14/81
COASTAL VALLEY--URBAN San Jose	6980	660	1/1/81-4/2/82*
COASTAL VALLEY--RURAL Santee	6820	002	10/9/75-12/6/75
Gilroy	7260	650	1/1/81-4/2/82*
CENTRAL VALLEY--URBAN CSCB (California State College, Bakersfield)	0520	021	8/5/77-10/24/77
CHP (California Highway Patrol office, Sacramento)	8840	026	9/24/76-12/15/76
CENTRAL VALLEY--RURAL Lab (Caltrans Laboratory, Sacramento)	6580	008	3/6/76-6/28/76
MOUNTAIN--RURAL** Mammoth Lakes	4760	101	1/15/81-5/13/81

* Two winter seasons monitored.

** No urban sites in the mountain category.

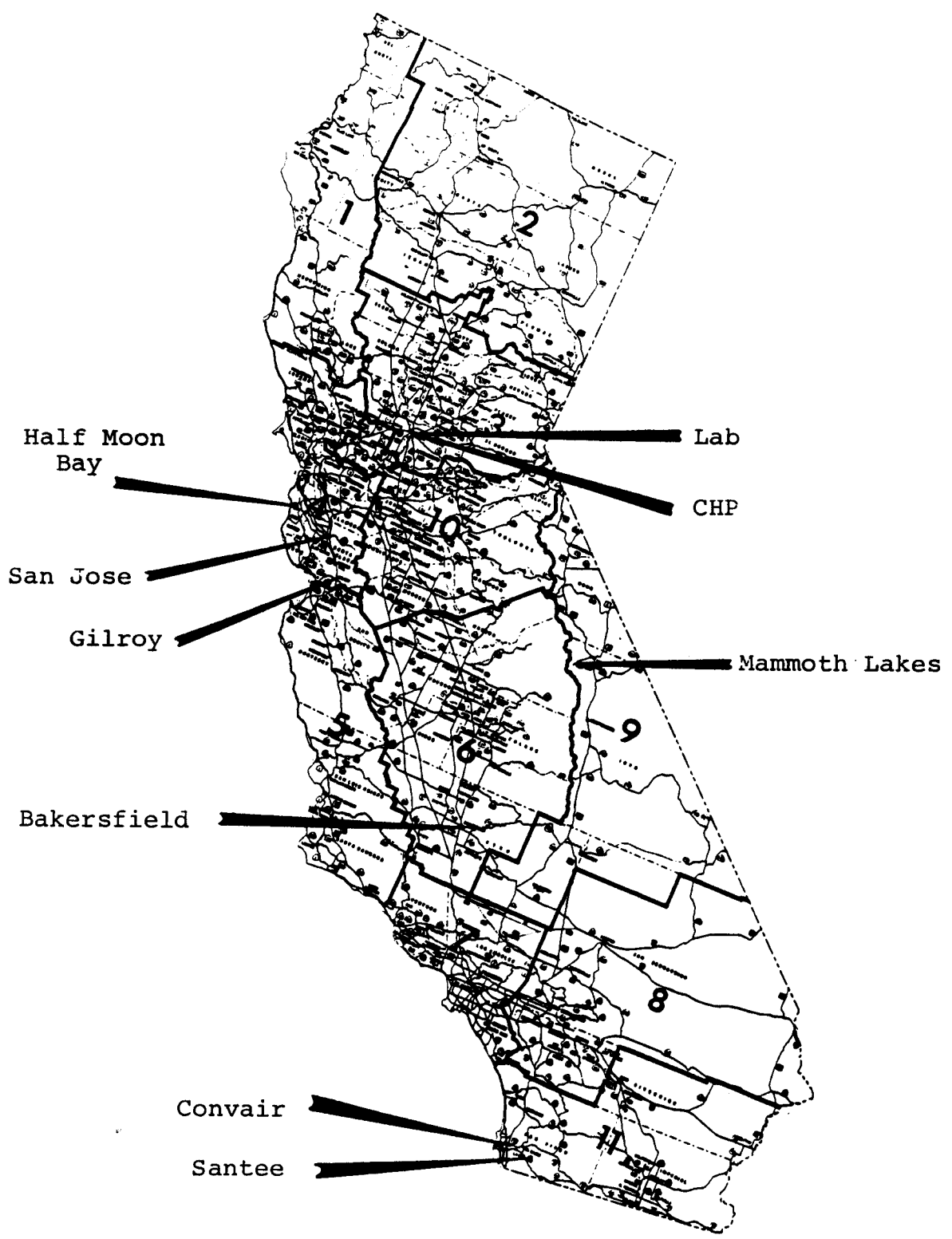


FIGURE 5-1. Meteorological Monitoring Sites for Developing Worst Case Meteorology Criteria.

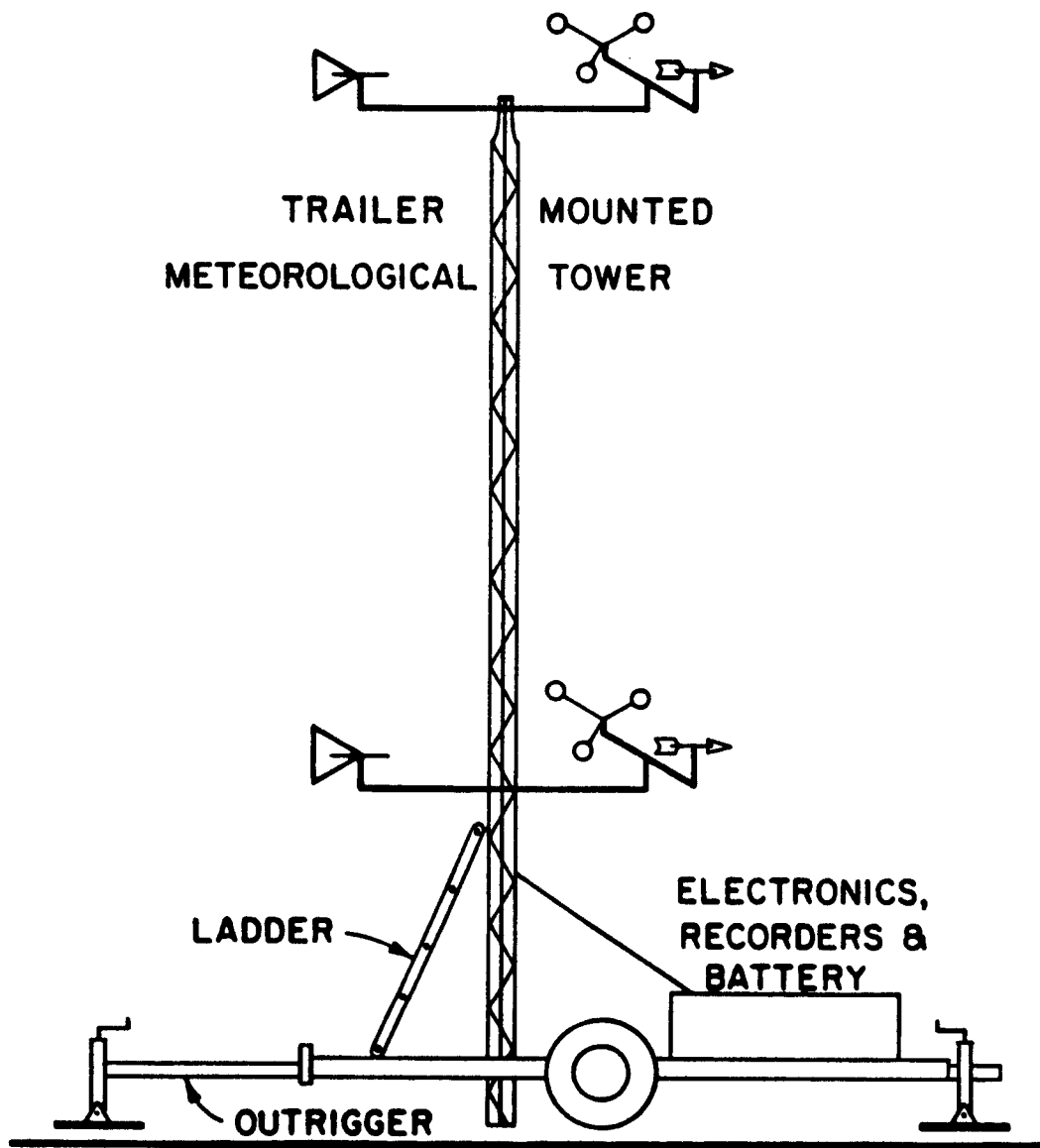


FIGURE 5-2. Typical Trailer Mounted Meteorological Tower

Each tower was equipped with a horizontal wind vane, two-cup anemometers, and two self-aspirated temperature sensors. Wind speed was recorded using Climet model WS-001-1 anemometers that have a threshold of 0.27 m/s and are accurate to one percent or 0.06 m/s (whichever is greater) over a range of 0.27 to 40 m/s. Climet model WD-012-30 wind direction transmitters were used on each tower. These sensors have a threshold of 0.33 m/s and are accurate to $\pm 3^\circ$. Ambient temperature was monitored by Climet model 015-3 thermistor sensors with a range of -30 to +50 $^\circ\text{C}$ and an accuracy of $\pm 0.15^\circ\text{C}$.

Each tower contained strip chart recorders and a Datel data logger that digitally recorded the aerometric data on cassette tape. Readings were recorded on tape once per minute by the data logger. The taped data were averaged for 1-hour periods during subsequent data reduction by a minicomputer. Printed copies were generated and magnetic tapes of the data were transferred to the Caltrans AQDHS aerometric data bank.

Minicomputer processing of wind direction included computing the hourly average standard deviation of the wind direction, referred to as sigma theta. This is a new input parameter needed by the CALINE4 dispersion model. The cassette tapes from the older sites were not analyzed for sigma theta when they were originally processed and were no longer available for updated processing. Sigma theta was estimated for these sites using the original strip charts by dividing the range of wind directions over each 1-hour period by six(4,5).

Another important model input, Pasquill Stability Class, was not measured directly nor was it determined during the original data reduction. However, stability class has

been related to the Bulk Richardson Number by Golder(6). This relationship was used to determine stability class from the measured wind speed and temperature data.

6. DEVELOPMENT OF A METEOROLOGICAL SEVERITY INDEX

The meteorological severity index (MSI), was developed to indicate the potential for pollutant levels given the combined effects of wind speed, directional variability, stability class, and temperature. This index was used as a screening device to identify meteorological scenarios that would likely promote high pollutant levels at receptors near a roadway. It provided an objective way to evaluate the real-world meteorology in terms of the anticipated model response.

The MSI was developed from CALINE4 predictions of CO concentrations for an assumed standard site geometry and varying meteorology. A functional relationship between meteorology and predicted CO level was derived by multiple regression analysis.

Table 6-1 shows the CALINE4 inputs that were used to develop the MSI. All runs used one receptor and a single highway link with a constant source strength. The receptor was offset 30 m from the midpoint of the 2 km long, 30 m wide link. Meteorological variables started with the limiting values suggested in the CALINE4 User Instructions(1) and were then changed by increments shown in Table 6-1 over a range of typical conditions. The model generated a set of 180 CO predictions for all the combinations of conditions summarized in Table 6-1. The results were normalized by dividing all results by the highest computed concentration.

A functional relationship between the meteorological variables and the model results was derived using stepwise multiple linear regression. Individual variables were studied as linearly transformed exponential, logarithmic,

Table 6-1. CALINE4 Inputs for MSI Development.

SITE CONSTANTS

Receptor Location : x=30 m, y=0 m, z=1.8 m
Link Location : x₁=0 m, y₁=1000 m
 x₂=0 m, y₂=-1000 m
Link Description : height=0 (at-grade), width=30 m
Traffic Volume : 5000 VPH
Emission Factor : 20 grams/vehicle-mile
Mixing Height : 1000 m
Surface Roughness : 50 cm
Settling Velocity : 0 m/s
Deposition Velocity : 0 m/s
Ambient Temperature : 25 °C
Ambient CO : 0 ppm

METEOROLOGICAL VARIABLES

Wind Speed : 0.5, 1, 2, 4, 6, & 10 m/s
Stability Class : Classes A-G (input as 1-7)
Sigma Theta : 5, 10, 15, 25, 40, & 75 degrees
Wind Direction : worst case wind angle

and power functions. In addition, interactions between individual meteorological variables were evaluated. The resulting best fit equation is as follows:

$$MSI = a \left\{ .085 - \frac{.0093}{u} + .018(k) + \frac{.55}{(\sigma_{\theta} \cdot 2)(u)} \right\}, \quad (6-1)$$

$$\text{where } a = \frac{(T + 100)}{(1.754(T+100) - 74.91)}, \quad (6-2)$$

T = temperature ($^{\circ}$ F)

u = wind speed (m/s), σ_{θ} = sigma theta (degrees), and

k = Pasquill Stability Class (1=A, 7=G).

Equation 6-1 shows that high MSI levels (i.e. concentrations) are caused by low winds, low sigma theta, and stable atmospheric conditions. The MSI will approximately equal unity if the worst case model limits of 0.5 m/s wind speed, 5° sigma theta and "G" stability are used in the equation with a temperature of 0° C.

The MSI correlates best with the sigma theta/wind speed interaction term. This term incorporates the effects of both dilution and horizontal spreading, the primary mechanisms used in CALINE4 to model pollutant dispersion. The correlation coefficient for the interaction term exceeds 0.97. It increases only slightly to 0.98 when the other terms in Equation 6-1 are included. These secondary terms represent less important dispersion mechanisms. The reciprocal wind speed term is attributable to the residence time algorithm in CALINE4 that increases initial vertical dispersion at low wind speeds. The dilution effect, also proportional to the reciprocal wind speed, is a much more dominant effect. Stability class is no longer a critical variable because CALINE4 now estimates horizontal dispersion directly from sigma theta and

adjusts near-roadway stability for vehicle-induced mechanical and thermal turbulence.

The temperature term shown in Equation 6-2 represents the effect of temperature on CO emissions. Emission factors for CO were generated by running the EMFAC6D program (California's version of MOBILE2) (7). Percent hot and cold starts were estimated based on a New Jersey field study(8). The vehicle mix was assumed as 82.5% light-duty auto, 12.2% light-duty truck, 1.4% medium-duty truck, 1.4% heavy-duty gasoline, 1.5% heavy-duty diesel, and 1.0% motorcycles. Vehicle speed was assumed to be 55 mph and emission rates were generated for 1985. Regression analysis yielded Equation 6-2 for various temperature values.

Sensitivity of the MSI to changes in site geometry typically varied less than 10% from the results using the standard site geometry. Model runs involving perturbation of one site geometry input at a time were made for all of the meteorological conditions listed in Table 6-1. High and low extremes of receptor distance, link length, and mixing zone width were studied. Depressed and bridge sections were analyzed, also. The MSI consistently provided a good indicator of expected air quality impacts for all conditions.

The MSI is most appropriate for wind speeds equal to or above the 0.5 m/s limiting value recommended in the CALINE4 user instructions(1). Though this is somewhat higher than the threshold of the instruments used in this study (approximately 0.3 m/s), the relationship of meteorological factors to the MSI was assumed to be consistent for all wind speeds. This difference had no effect since the analysis for the 1-hour and 8-hour CO standards eventually involved only data above instrument threshold.

7. DETERMINING WORST CASE METEOROLOGICAL SCENARIOS
FOR MAXIMUM 1-HOUR AVERAGED CO CONCENTRATIONS

A. Introduction

The MSI was used to develop worst case scenarios based on the joint probability distributions of wind speed and sigma theta. These scenarios were selected using probabilities consistent with the wording of the National Ambient Air Quality Standards (NAAQS). Limiting conditions were imposed for cases where the probabilistic method predicted wind conditions that were below either instrumentation thresholds or CALINE4 model limits. A technique to establish worst case temperature was developed that uses readily available National Weather Service data. Worst case stability classes were estimated by examining high-MSI episodes.

The hourly averages in the data were evaluated by discrete time-of-day periods. The four time periods were morning (0600-1000), midday (1000-1700), evening (1700-2100), and nocturnal (2100-0600). By using discrete time periods, the meteorological scenarios can be matched to appropriate ambient concentrations and traffic(9,10). Also, by dividing the meteorological data into time-of-day categories, results were expected to follow a uniform, unimodal distribution that could be modeled with reasonable accuracy.

The histograms of wind speed and sigma theta at different locations were similar, but not identical. Figures 7-1 and 7-2, for Mammoth and Half Moon, are representative of the types of distribution exhibited for all sites. Distributions were skewed positively by extreme high values at all locations. This is typical for measures of

natural phenomena, such as wind speed or pollutant concentration, where the lower limit is bounded by zero.

As expected, there were significant differences in the histograms between time-of-day periods. Figures 7-1 and 7-2 show distributions of wind speed and sigma theta for the nocturnal and midday time periods. Higher wind speeds and lower sigma theta during midday contrast markedly with the nocturnal distributions. The midday conditions typify the unstable atmospheric mixing that prevails during daylight hours. During nocturnal periods, wind speeds are less and sigma theta varies over a much wider range than at other times.

These histograms provide an indication of the wind speed and sigma theta patterns at each site. However, they do not yield any information about possible dependence between the variables, or their relation to high-MSI events. A joint probability analysis must be made to address these issues.

B. Probabilistic Analysis

The MSI could not be used directly to determine worst case combinations of wind speed and sigma theta from the histograms. The MSI represents a deterministic relationship between model results and meteorological inputs, but does not account for the dependence between wind speed and sigma theta that has been observed by others(11). Therefore, a mathematical description of the wind speed/sigma theta relationship had to be linked with the MSI to derive the worst case, 1-hour meteorological scenarios.

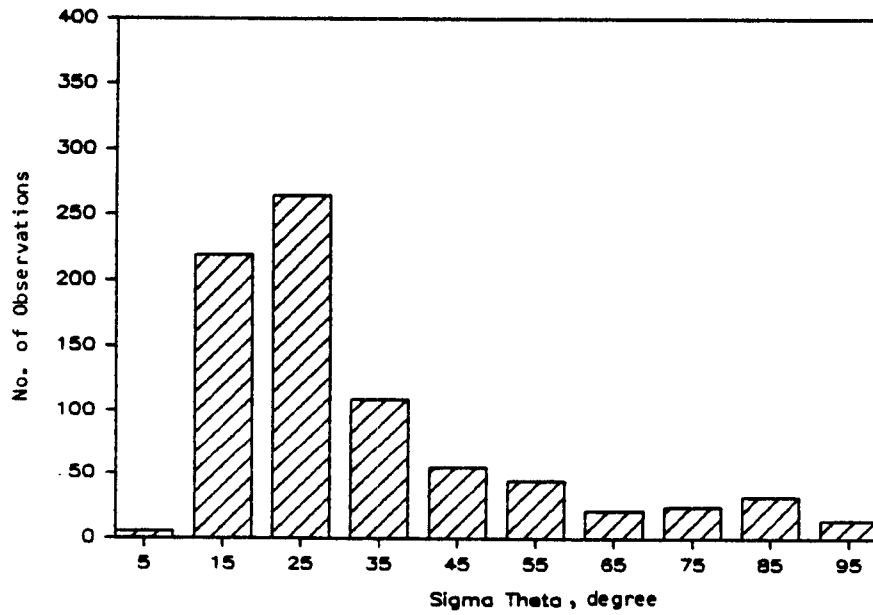
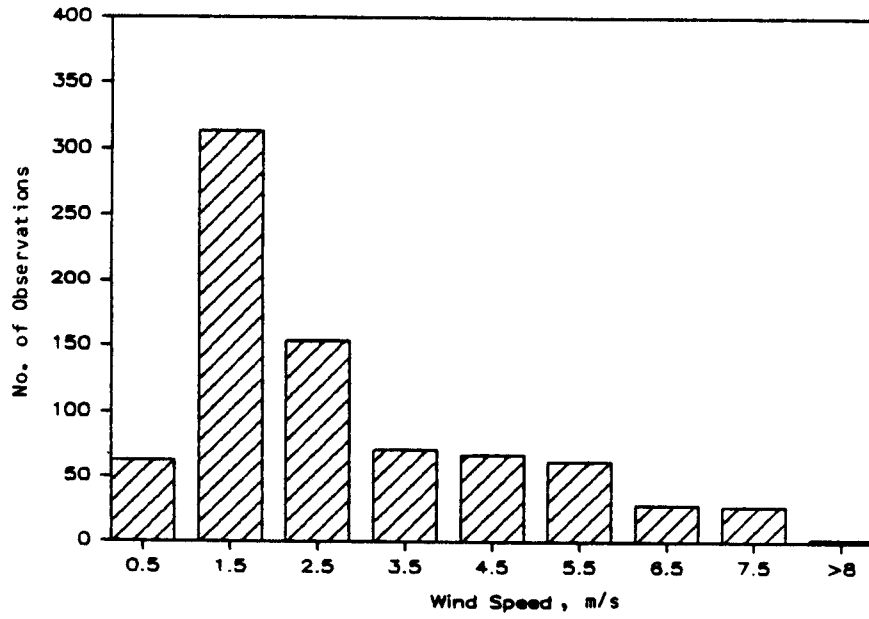


FIGURE 7-1(a). Wind Speed and Sigma Theta Histograms: Mammoth, Nocturnal Period (n = 787).

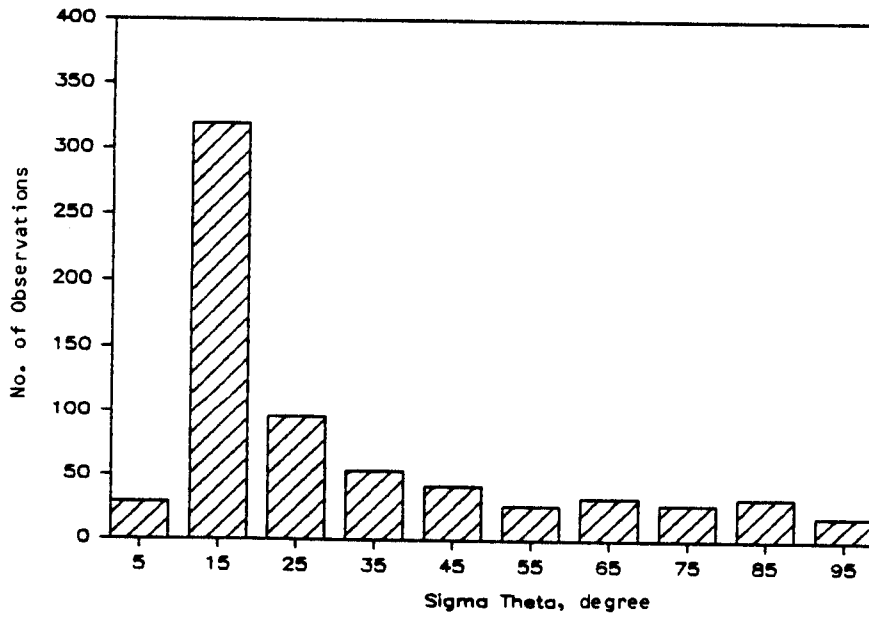
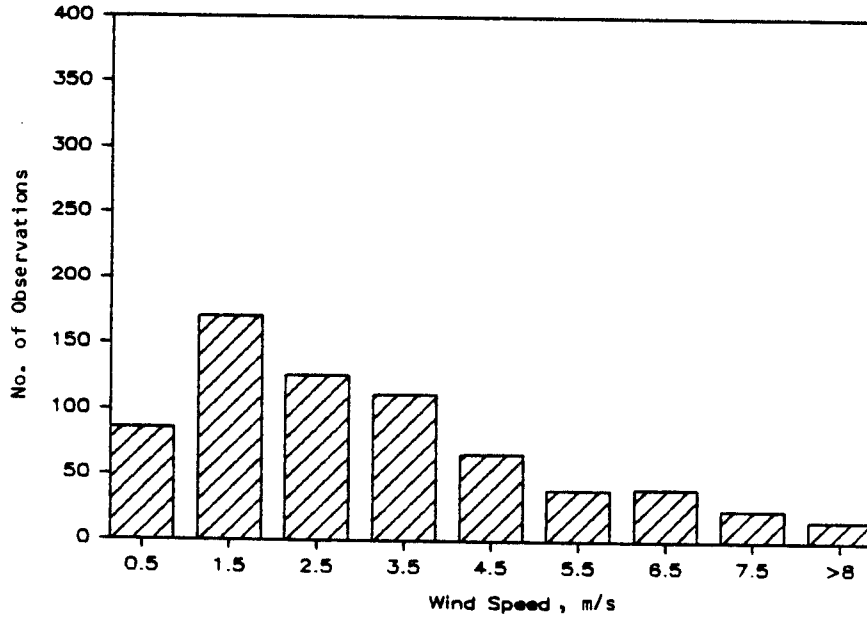


FIGURE 7-1(b). Wind Speed and Sigma Theta Histograms:
Half Moon, Nocturnal Period (n = 680).

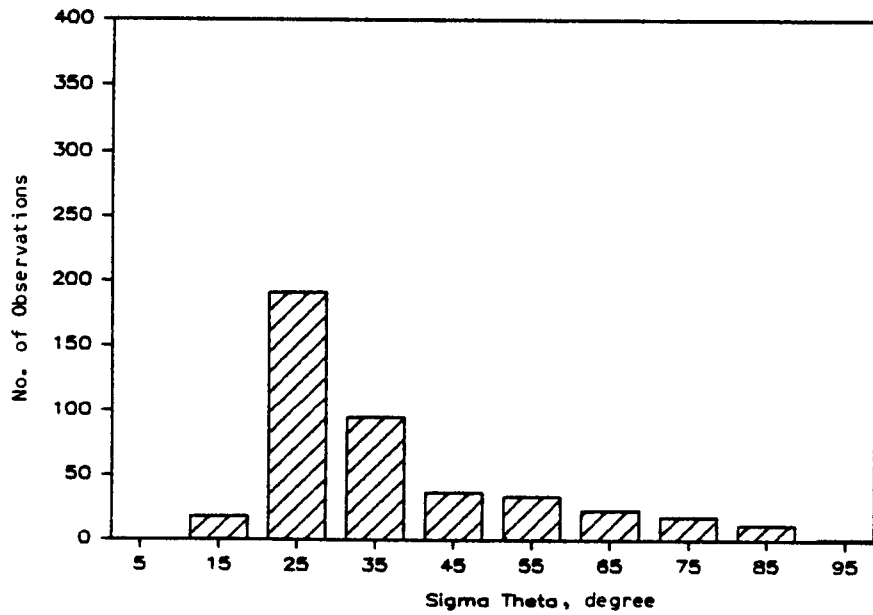
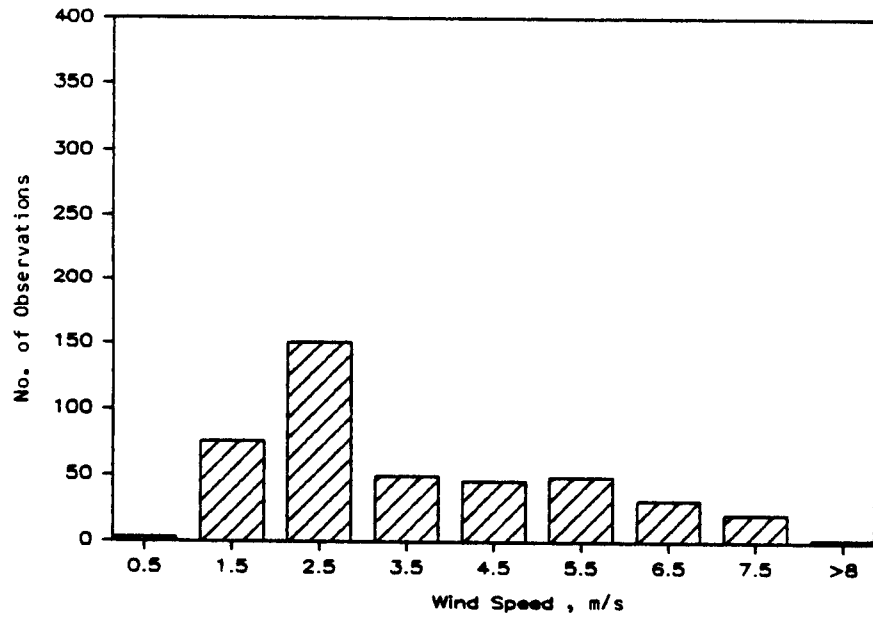


FIGURE 7-2(a). Wind Speed and Sigma Theta Histograms: Mammoth, Midday Period (n = 429).

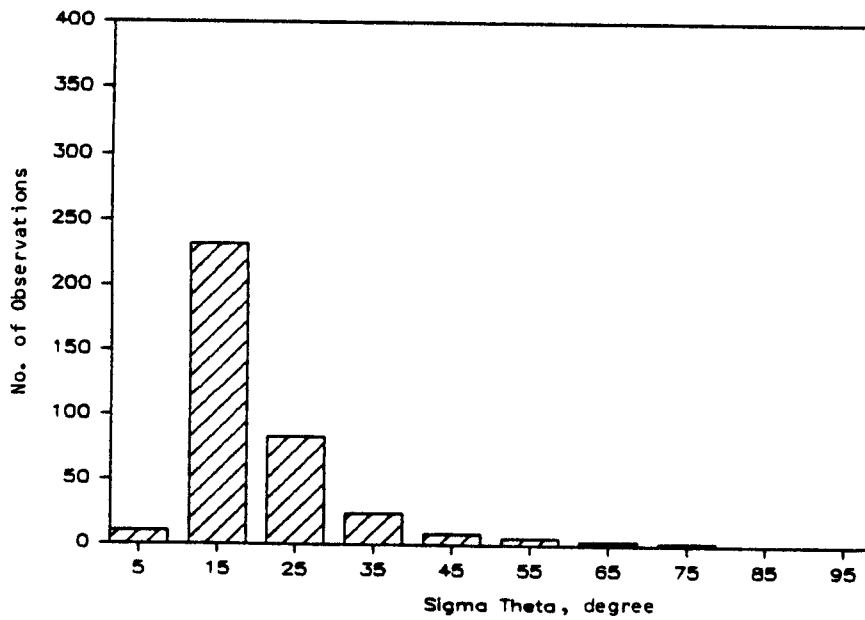
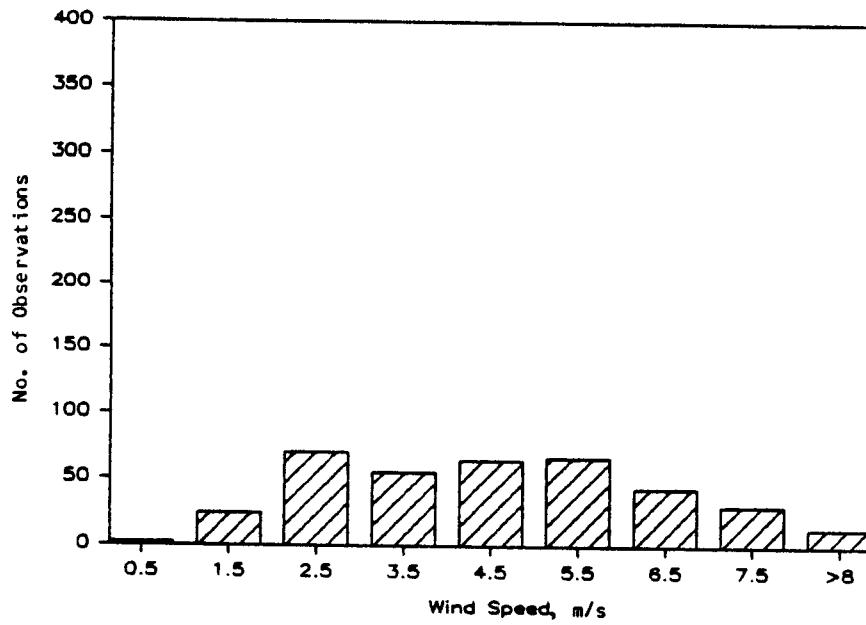


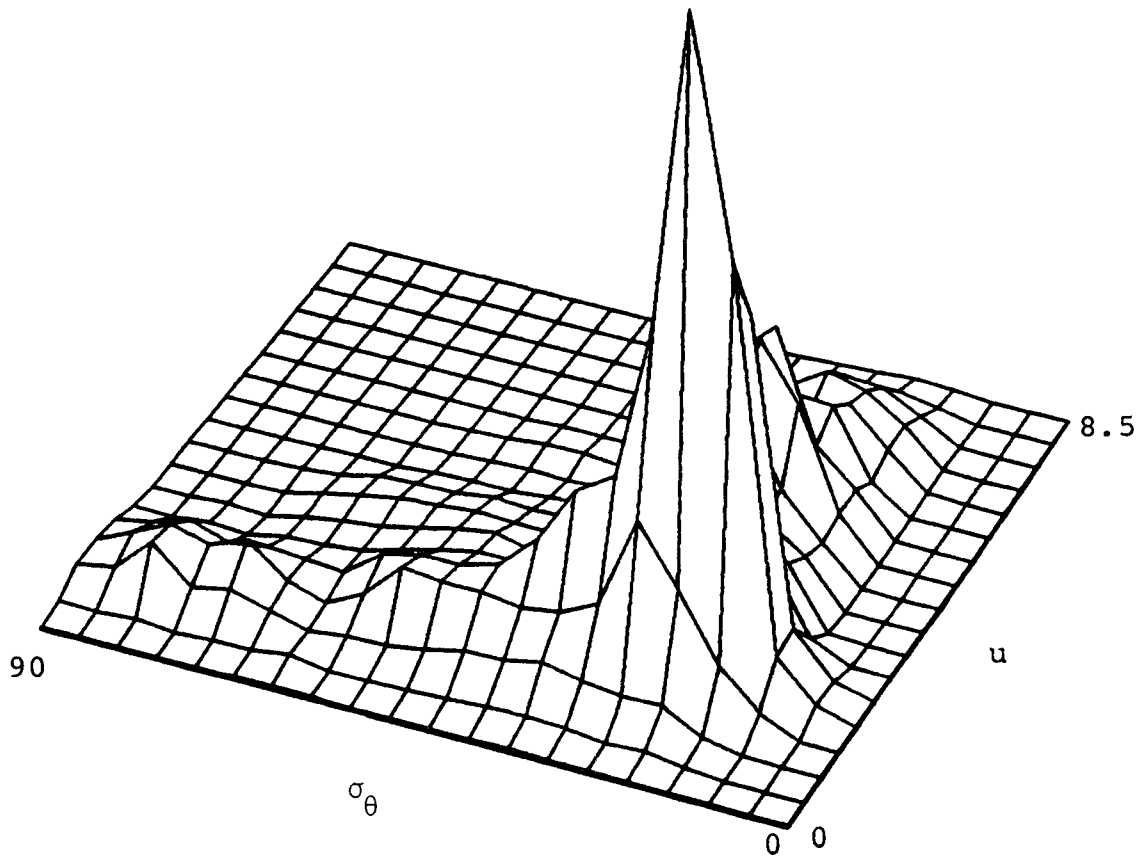
FIGURE 7-2(b). Wind Speed and Sigma Theta Histograms: Half Moon, Midday Period (n = 367).

Previous research has shown that sigma theta values increase when wind speeds decrease(11). For the most part, wind data collected during this study followed this general relationship. However, there was substantial scatter of the sigma theta measurements during low wind speeds for all sites and all time-of-day periods. This increased scatter is attributable to wind meander caused by large-scale turbulence during locally calm conditions(11).

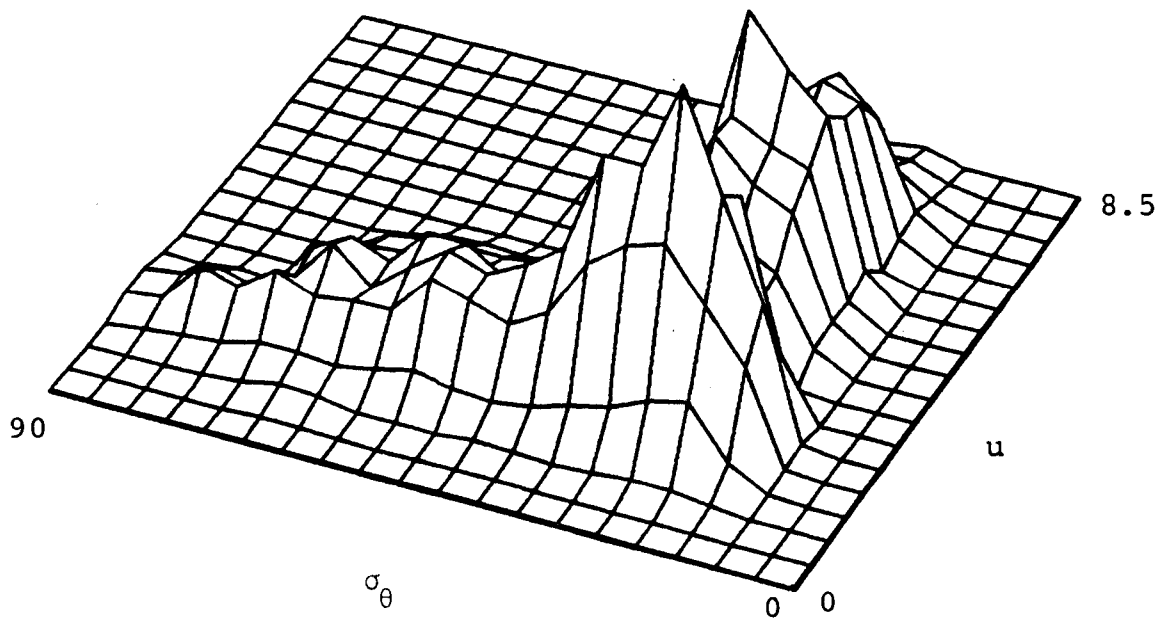
To explore the relationship between sigma theta and wind speed, joint frequency distributions were established. A joint frequency distribution represents the probability of two events occurring simultaneously. Frequency distributions for individual variables, such as those shown in Figures 7-1 and 7-2, are called marginal distributions. The joint distribution is a combination of these marginal distributions.

The joint wind speed/sigma theta distributions for Mammoth and Half Moon are shown in Figures 7-3 and 7-4. As with Figures 7-1 and 7-2, the patterns are typical of the distributions at all the monitoring sites, though distribution parameters such as mean and standard deviation vary from one site to another. Wind speed (u), sigma theta (σ_θ), and number of observations are plotted on the x, y, and z axes, respectively. The scale for number of observations is proportional to that shown in Figures 7-1 and 7-2 for corresponding sites and periods.

Figures 7-3 and 7-4 present a three-dimensional picture of the frequencies of occurrence (by dividing observations in a specified range by total observations) for any combination of wind speed and sigma theta. At low wind speeds, high values for sigma theta are more likely than

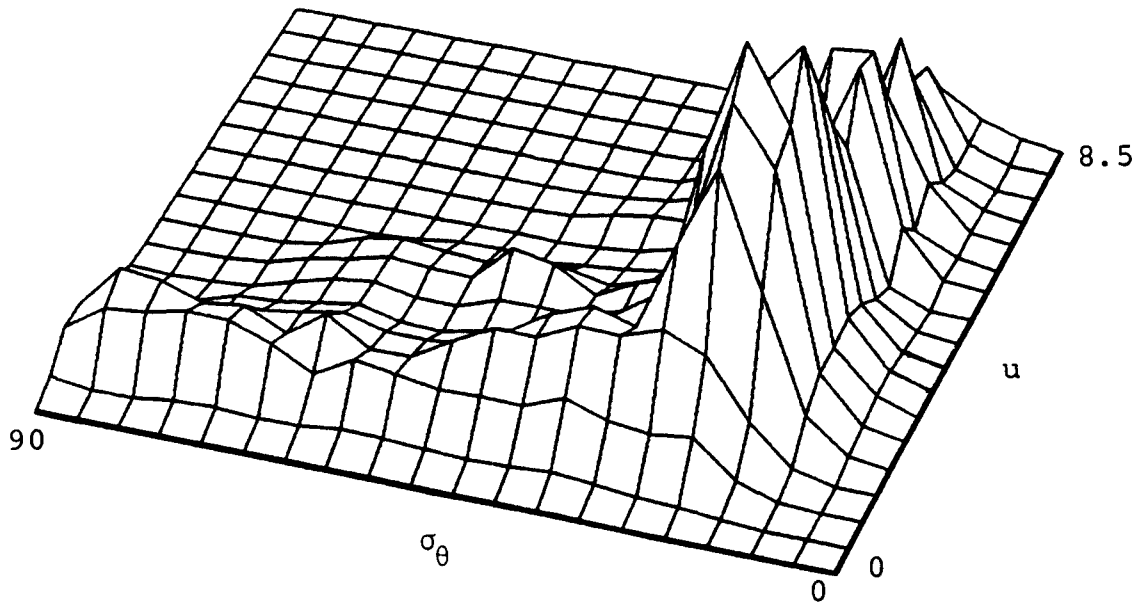


(a) SIGMA THETA VS WIND SPEED - MAMMOTH, NOCTURNAL

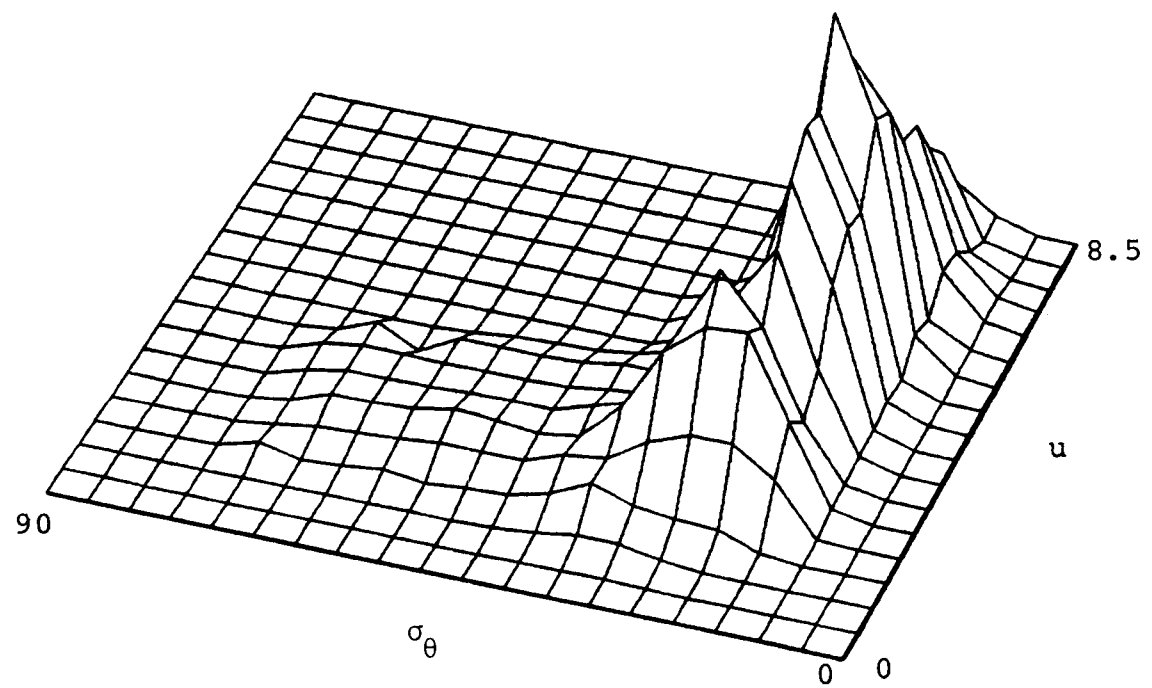


(b) SIGMA THETA VS WIND SPEED - MAMMOTH, MIDDAY

FIGURE 7-3. Joint Probability Distribution of Sigma Theta with Wind Speed at Mammoth Lakes During (a) Nocturnal and (b) Midday Periods.



(a) SIGMA THETA VS WIND SPEED - HALFMOON, NOCTURNAL



(b) SIGMA THETA VS WIND SPEED - HALFMOON, MIDDAY

FIGURE 7-4. Joint Probability Distribution of Sigma Theta with Wind Speed at Half Moon Bay During (a) Nocturnal and (b) Midday Periods.

low values. At high wind speeds the reverse is true. This dependence, along with the marginal probabilities, determines the shape of these distributions.

The joint probability distributions were used with a second annual maximum criterion, consistent with the wording of the NAAQS, to determine peak MSI combinations of wind speed and sigma theta for each site/time period combination. Similar methods have been used by other researchers studying environmental processes(12,13,14). The technique is analogous to a hydrologist's flood frequency analysis for determining peak flow during a 50 or 100-year storm. The same concept of selecting a probability consistent with a chosen recurrence interval and applying it to an observed frequency distribution is used. In this case, however, the analysis is complicated by the presence of two dependent variables.

The NAAQS allow one exceedance of the CO standard per year. As a result, finding the meteorological conditions that correspond to the second annual maximum is necessary to determine compliance with the CO standard. If all 1-hour average CO measurements recorded in a year are ranked in descending order, the second annual maximum concentration corresponds to the second highest hour in the ranking. Since this is a finite data set, the second highest value can be represented by the percentile (used as probability) calculated as shown below(12):

$$P_2 = 100\% \cdot [1 - ((N-1)/N)] , \quad (7-1)$$

where N represents the total number of hours for a time period in entire year. The denominator in the last term would be N+1 if an infinite upper tail (no maximum wind speed or sigma theta) were assumed for the distribution.

However, a finite tail was assumed since there is a limit to the highest wind speed and sigma theta values that are likely to occur. Computed values of P_2 for each time-of-day period are shown in Table 7-1.

A joint probability density function (PDF) is typically defined as the product of the marginal probabilities. However, this assumes that the variables are independent of each other. The general form of this relationship is shown in Equation 7-2:

$$P(x,y) = P(x) \cdot P(y) , \quad (7-2)$$

where $P(x,y)$ is the joint PDF and $P(x)$ and $P(y)$ are the marginal density functions(15,16). Restating Equation 7-2 with the appropriate variables being studied here yields the following equation:

$$P(u, \sigma_{\theta}) = P(u) \cdot P(\sigma_{\theta}) . \quad (7-3)$$

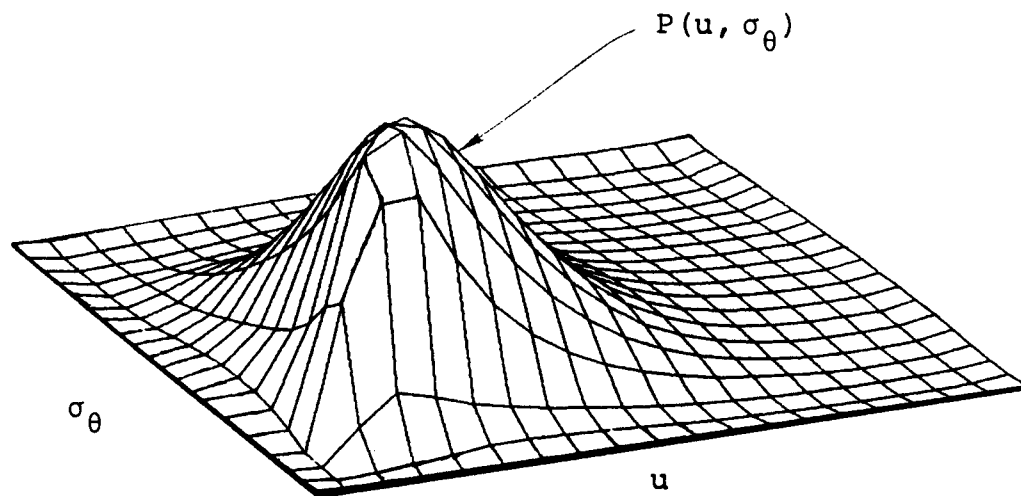
The relation expressed in Equation 7-3 is shown graphically in Figure 7-5. If wind speed and sigma theta are independent of each other, the "surface" shown in Figures 7-3 and 7-4 would represent $P(u, \sigma_{\theta})$. The marginal functions $P(u)$ and $P(\sigma_{\theta})$ lie in the "x-z" and "y-z" planes, respectively.

When variables are not independent, a special correlation parameter must be included in the joint density function. This parameter, the correlation coefficient ρ , is a measure of mutual dependence of the variables and is defined as:

$$\rho = \frac{\text{covar}(x,y)}{s_x \cdot s_y} \quad (7-4)$$

Table 7-1. Probability, P_2 , for Time Periods.

Time Period	Probability, P_2
Morning	0.00274
Midday	0.00157
Evening	0.00274
Nocturnal	0.00122



SIGMA THETA VS WIND SPEED ($\rho = 0$)

FIGURE 7-5. Surface Described by the Joint Probability Density Function (PDF) in Equation 7-3.

where s_x and s_y are respective standard deviations. The covariance of x and y is computed using Equation 7-5:

$$\text{covar}(x,y) = \sum_{i=1}^n (x_i - \bar{x})(y_i - \bar{y}) / (n-1). \quad (7-5)$$

Substituting u and σ_θ into Equation 7-5 yields the following expression:

$$\text{covar}(u,\sigma_\theta) = \sum_{i=1}^n (u_i - \bar{u})(\sigma_{\theta i} - \bar{\sigma}_\theta) / (n-1). \quad (7-6)$$

The correlation coefficient ranges from -1 to +1 indicating perfect inverse and direct dependence, respectively. The variables are assumed to be independent if the correlation coefficient is zero(16,17). Note that ρ equals zero in Figure 7-5 due to independence.

Mutual dependence between wind speed and sigma theta was found from the correlation coefficients calculated for each site and time-of-day period. Dependence was not totally unexpected since Figures 7-3 and 7-4 show a systematic tendency towards low sigma theta values at high wind speeds (greater than about 2 m/s). Table 7-2 shows the correlation coefficients computed for each site. The negative sign of the correlation coefficient in all entries but one is caused by the inverse dependence between wind speed and sigma theta.

C. Curve-Fitting Using a Lognormal Function

A lognormal distribution was selected to model the marginal probability distributions of wind speed and sigma theta. Lognormal models have been applied successfully to other similar environmental variables(13,14,18). They permit only positive values and have a "tail" tapering off as values increase (positive skewness). The distributions

Table 7-2. Correlation Coefficients Relating
Wind Speed and Sigma Theta Dependence.

Geographic Location	Time Period			
	Morning	Midday	Evening	Nocturnal
Coastal				
Convair	-.362	-.421	-.378	-.206
Half Moon	-.797	-.713	-.758	-.705
Coastal Valley				
San Jose '81	-.607	-.786	-.501	-.494
San Jose '82	-.656	-.824	-.545	-.567
Gilroy '81	-.639	-.837	-.766	-.658
Gilroy '82	-.713	-.772	-.672	-.633
Santee	-.409	-.551	-.385	-.042
Central Valley				
CSCB	-.412	-.774	-.185	-.444
CHP	-.347	-.627	-.288	-.275
Lab	.074	-.339	-.014	-.144
Mountain				
Mammoth	-.400	-.334	-.454	-.296

shown in Figures 7-1 through 7-4 conform reasonably well to the lognormal model.

Before describing the distribution-fitting analysis used in this study, a discussion of fundamental probability terminology may help the reader. The form of a normal, or Gaussian, probability density function for a random variable x is shown below:

$$p(x) = \frac{1}{\sigma\sqrt{2\pi}} e^{-(x-\mu)^2/2\sigma^2}, \quad (7-7)$$

where μ is the distribution mean value, and σ is the standard deviation of the distribution.

Equation 7-7 is a univariate PDF in x . If the probability that a value x_i lies between x_1 and $x_1 + \Delta x$ is represented by $P(x_1 < x_i < x_1 + \Delta x)$, then the probability is related to the PDF as follows:

$$p(x_i) = \lim_{\Delta x \rightarrow 0} \left\{ \frac{P(x_1 < x_i < x_1 + \Delta x)}{\Delta x} \right\} = \frac{dP}{dx}. \quad (7-8)$$

Equation 7-8 shows that the PDF is equal to the first derivative of the probability with respect to x . This means that the probability associated with $x_i = x_1$ is undefined and can not be determined directly from the PDF. This is not a problem, however, since the limiting probability P_2 (from Equation 7-1) is not to be exceeded.

Equation 7-7 can be expanded to study a two variable, or bivariate, normal PDF as shown below:

$$p(x,y) = \frac{e^{\left\{ \frac{-1}{2(1-\rho^2)} \left[\left(\frac{x-\mu_x}{\sigma_x} \right)^2 - 2\rho \left(\frac{x-\mu_x}{\sigma_x} \right) \left(\frac{y-\mu_y}{\sigma_y} \right) + \left(\frac{y-\mu_y}{\sigma_y} \right)^2 \right] \right\}}}{2\pi\sigma_x\sigma_y\sqrt{1-\rho^2}}, \quad (7-9)$$

where ρ is the correlation coefficient from Equation 7-4. Transforming the bivariate normal PDF (equation 7-9) into a bivariate lognormal (BLN) PDF in u and σ_θ yields Equation 7-10(16,19):

$$p(u, \sigma_\theta) = \frac{e^{\left\{ \frac{-1}{2(1-\rho^2)} \left[\left(\frac{u-m_u}{s_u} \right)^2 - 2\rho \left(\frac{u-m_u}{s_u} \right) \left(\frac{\sigma_\theta - m_{\sigma_\theta}}{s_{\sigma_\theta}} \right) + \left(\frac{\sigma_\theta - m_{\sigma_\theta}}{s_{\sigma_\theta}} \right)^2 \right] \right\}}}{2\pi s_u s_{\sigma_\theta} \sqrt{1-\rho^2}}, \quad (7-10)$$

Equation 7-10 incorporates the geometric mean (m) and geometric standard deviation (s) of the marginal distributions, and the coefficient of correlation (ρ) between sigma theta and wind speed. These parameters were computed for each site and time period and used as constants in the PDF. Equation 7-10 was then solved by iteration at uniform intervals of sigma theta and wind speed to generate a BLN PDF for each site/time period combination. This solution can be interpreted graphically as a "surface", shown in Figure 7-6, as was done for the simplified, independent case (Figure 7-5). However, Figure 7-6 shows the positive skewness of the marginal distributions and inverse dependence between wind speed and sigma theta apparent in the observed distributions (Figures 7-3 and 7-4).

Ideally, if Equation 7-10 adequately describes how wind speed and sigma theta vary jointly, probabilities computed by integrating this equation over a specific range of values should approximate the observed frequency distribution over the same range. The goodness-of-fit of the function to the data was tested based on this hypothesis.

D. Testing Goodness-Of-Fit

The Chi-squared statistic was used to evaluate goodness-of-fit of the BLN distributions. The first step in this statistical evaluation is to partition the observed and predicted frequencies into discrete ranges. Next, differences between observed and predicted frequencies are computed. The magnitude of these differences is then tested against the Chi-squared statistic. The efficiency of the test was increased by maintaining approximately equal numbers of occurrences in each cell and never allowing less than than 5 occurrences per cell(14,20,21).

Chi-squared test results in Table 7-3 show mixed agreement of the observed and predicted frequency distributions. However, each geographic category except mountain contains a data set that passed the Chi-squared test so it was assumed that the BLN PDF adequately characterizes the joint distribution of sigma theta and wind speed. It is likely that the effort to represent the data as lognormally distributed was confounded by serial correlation (the extent to which conditions during one period affect those in a later period). Further stratification and analysis would improve agreement between observations and predictions but were not warranted in this study.

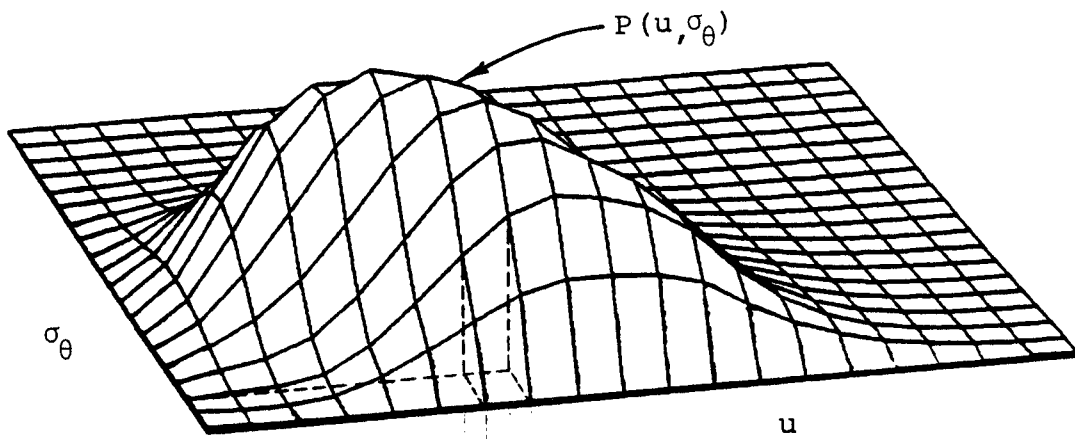
E. Worst Case Wind Speed And Sigma Theta

A worst case probability was determined using Equation 7-1 for each of the time periods at all sites. This probability was then used with the BLN PDF and MSI equations to select the worst case combination of wind speed and sigma theta. Figure 7-6 graphically represents this approach. It shows the surfaces that the MSI and BLN PDF functions

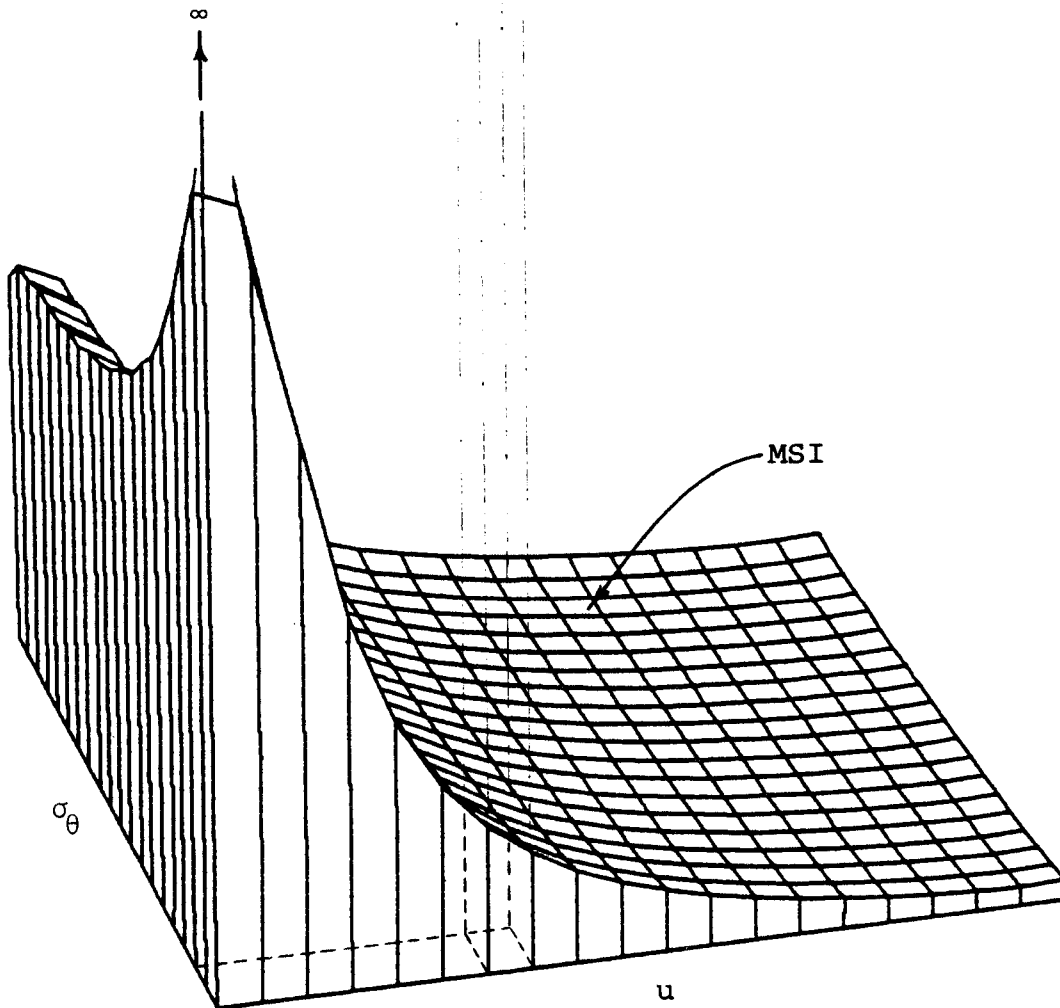
Table 7-3. Chi-Squared Statistic Test Results.

Geographic Location	Time Period			
	Morning	Midday	Evening	Nocturnal
Coastal				
Convair	2.2	11.6	6.4	26.4
Half Moon	27.6	44.9	46.9	42.3
Coastal Valley				
San Jose '81	6.7	7.4	18.6	16.7
San Jose '82	6.0	18.9	16.3	6.2
Gilroy '81	15.3	11.9	14.1	9.9
Gilroy '82	4.9	12.5	5.6	5.9
Santee	26.6	15.7	35.3	35.3
Central Valley				
CSCB	7.2	6.6	72.9	8.1
CHP	10.8	22.2	16.2	35.4
Lab	4.1	9.7	3.4	42.4
Mountain				
Mammoth	20.1	65.0	43.6	42.9

Note: Critical Chi-Squared value = 11.1 at the 95% confidence interval.



SIGMA THETA VS WIND SPEED ($\rho < 0$)



MSI As A Function of Wind Speed & Sigma Theta

FIGURE 7-6. Surfaces Described by BLN PDF and MSI Functions.

describe. The worst case combination of wind speed and sigma theta (from the BLN PDF) can be found at the "highest" point on the MSI surface that coincides with the given worst case probability.

Worst case wind speed and sigma theta for all site-time period combinations are shown in Table 7-6 (page 47) along with the worst case temperature and stability class recommendations (to be discussed shortly). Selection of these worst case scenarios involved practical consideration of the meteorological conditions that lead to high CO, and the operational limits of the CALINE4 model. For example, in those instances where the predicted worst case wind speed was less than the 0.5 m/s limit imposed by CALINE4(1), the model threshold was used as a lower boundary. In several other instances, extremely high values of sigma theta were predicted. These were usually associated with major shifts in wind direction or low wind speeds at or near instrument threshold. Therefore, predicted worst case sigma theta values that were more than 45 degrees were assumed to not represent worst case scenarios.

F. Worst Case Stability Class And Temperature

1). Stability Class

Sensitivity studies indicate that CALINE4 is less sensitive to stability class than its predecessor, CALINE3(1,2). Though stability class can substantially affect model predictions when traffic volumes are low, high CO levels are not typically associated with low traffic. The minimal influence of stability class is evident by its low coefficient in the MSI expression (Equation 6-1).

Worst case stability conditions were extracted from each data set by examining hours when actual conditions were similar to the predicted worst case conditions. For the morning, evening and nocturnal time periods, "G" was the prevalent stability class at all sites. For midday periods, a variety of stability conditions was found at the sites. In accordance with the original Pasquill stability typing system, "D" stability was chosen as the worst case midday condition.

2). Temperature

Temperature is important for predicting worst case CO levels because of its effect on vehicle emissions. Colder temperatures lead to higher CO emissions, particularly during the cold start phase of vehicle operation (i.e. the first 505 seconds). A recent study of meteorological influences on CO levels found that temperatures as much as 30° F below the annual mean temperature were typical during occurrences of peak 1-hour CO levels(22). These lower temperatures are associated with emission factors that are 40% higher than those occurring at the annual mean temperature.

A method for deriving worst case temperature was developed by examining low temperature patterns in each geographic category and correlating these to readily available National Weather Service (NWS) data. Daily minimum temperatures from October through March were extracted from the project stations and compared to daily minimums at nearby NWS stations(23). Since more than 250 stations comprise the California NWS network, temperature data were available for locations close to the monitoring sites. Table 7-4 shows the project monitoring sites and corresponding NWS sites that were chosen.

Table 7-4. National Weather Service and Air
Quality Data Handling System Sites.

Coastal			
Half Moon	(NWS 3714-04)	Half Moon	(AQDHS 3090-101)
Coastal Valley			
Gilroy	(NWS 3417-04)	Gilroy	(AQDHS 7260-650)
San Jose	(NWS 7821-04)	San Jose	(AQDHS 6980-660)
Mountain			
Mono Lake	(NWS 5779-03)	Mammoth	(AQDHS 4760-101)

The lowest temperatures that occurred during the highest MSI events for each time-of-day period were examined. These temperatures were then compared to the NWS temperature data for the same winter season. Preliminary study showed that January mean minimum temperatures correlated best to high-MSI temperatures. Figure 7-7 shows high-MSI temperatures for the project sites plotted against January mean minimum temperatures at corresponding NWS sites for the same year. High-MSI temperatures typically exceed the January mean minimum temperature by 5° to 10° F for all time-of-day periods except nocturnal.

Modifying the January mean minimum temperature by adding a time-of-day adjustment factor resulted in the most effective technique for determining worst case temperatures. The factor for midday is 10° F. For morning and evening the factor is 5° F. No factor is used for the nocturnal period. These adjustments substantially improved correlation between January mean minimums and the high-MSI temperatures. However, substantial deviation between the adjusted NWS temperatures and the high-MSI measured temperatures still occurred in some instances.

The January mean minimum temperatures for the three years immediately preceding the high-MSI events were reviewed to check for better correlation to the high-MSI temperatures. Table 7-5 shows these January mean minimum temperatures with the lowest value for each site in parentheses. Much better agreement resulted when the adjustment factor was applied to these three-year minimums, as shown in Figure 7-8. This resulted in an average deviation of no more than 2° F for each geographic location. It was, therefore, concluded that the temperature adjustments should be based on the lowest January mean minimum temperature over a three year period.

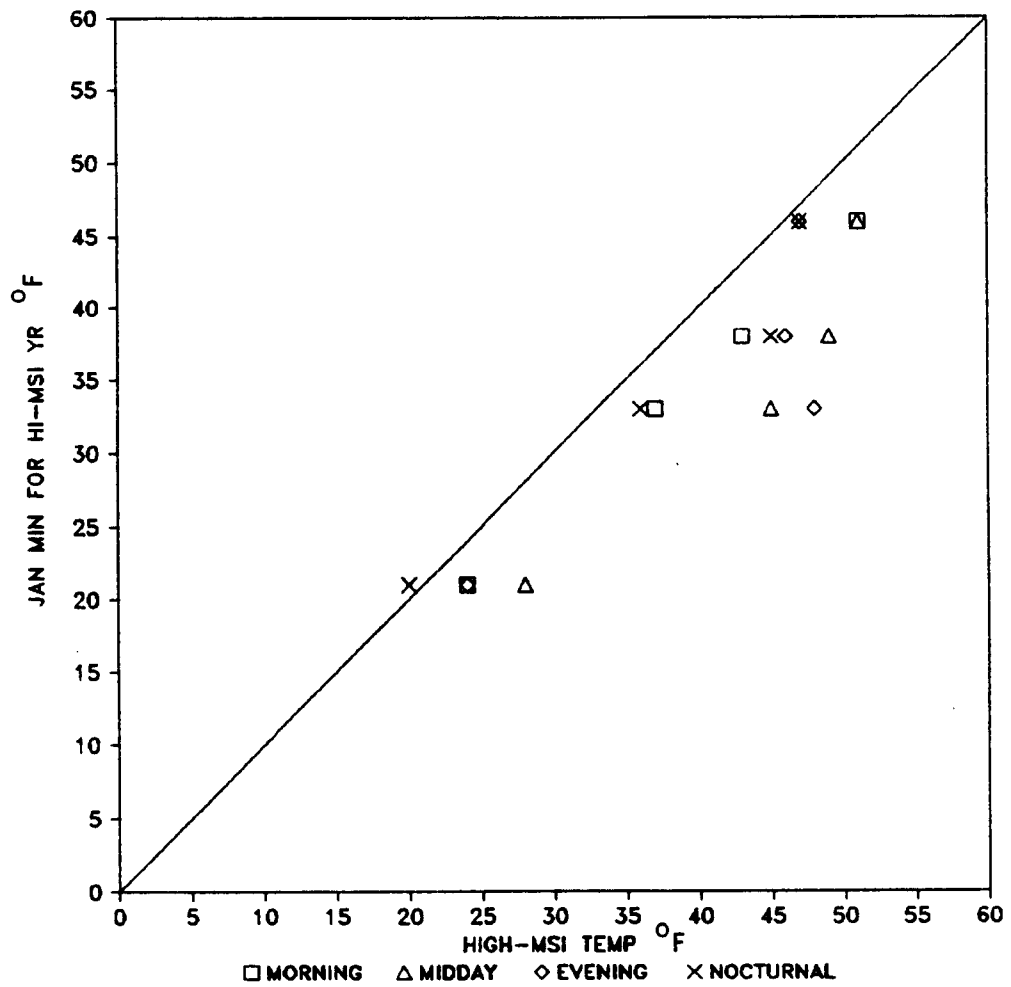


FIGURE 7-7. January Mean Minimum Temperatures Versus High - MSI Temperatures.

Table 7-5. January Mean Minimum Temperatures Showing Minimums for Three Years in Parentheses, °F.

Site	1978	1979	1980	1981
Half Moon	47	(42)	44	--
Mammoth (Mono)	20	(18)	23	--
Gilroy	--	(35)	42	38
San Jose	--	(41)	45	46

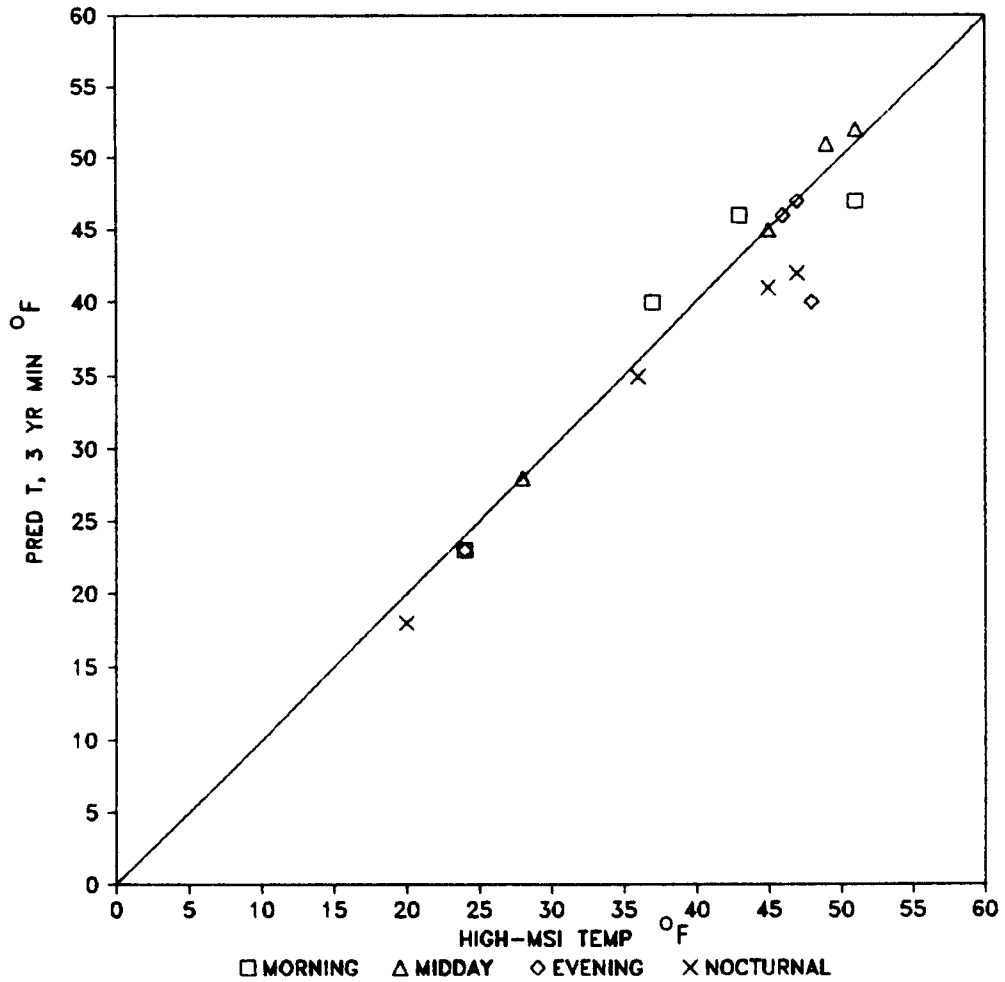


FIGURE 7-8. Predicted Temperatures Using Adjustment Factor Versus High - MSI Temperatures.

G. 1-HOUR WORST CASE METEOROLOGY

Table 7-6 lists the values for wind speed, sigma theta, stability class, and temperature that are recommended for 1-hour worst case analyses when no site-specific meteorological data are available. Appropriate values from Table 7-6 can be input to CALINE4 to estimate worst case CO impacts for any geographic category and time period. No consistent differences between urban and rural data were detected in development of these criteria. Therefore, no distinction is made between urban and rural land use.

Table 7-6. Suggested Worst Case 1-Hour Meteorological Scenarios.

Geographic Location	Wind Speed	Sigma Theta	Stab. Class	Δ Temp.
MORNING				
(0600-1000)				
Coastal	0.5	10	"G"	+5
Coastal Val.	0.5	20	"G"	+5
Central Val.	0.5	5	"G"	+5
Mountain	0.5	30	"G"	+5
MIDDAY				
(1000-1700)				
Coastal	1.0	25	"D"	+10
Coastal Val.	0.6	30	"D"	+10
Central Val.	0.5	20	"D"	+10
Mountain	0.9	30	"D"	+10
EVENING				
(1700-2100)				
Coastal	0.5	10	"G"	+5
Coastal Val.	0.5	10	"G"	+5
Central Val.	0.5	5	"G"	+5
Mountain	0.5	30	"G"	+5
NOCTURNAL				
(2100-0600)				
Coastal	0.5	5	"G"	0
Coastal Val.	0.5	15	"G"	0
Central Val.	0.5	10	"G"	0
Mountain	0.5	20	"G"	0

Note: Wind speed is in m/s, sigma theta in degrees, and Δ temperature in degrees Fahrenheit. Add Δ temperature to lowest January mean minimum temperature over three year period.

8. PREDICTING WORST CASE 8-HOUR AVERAGE CO CONCENTRATIONS

A. Introduction

Hourly changes in meteorology and traffic invariably cause 8-hour CO concentrations to be less severe than 1-hour values. For example, fluctuating wind directions alter transport and enhance horizontal diffusion of pollutants. Changes in ambient temperature can cause a substantial drop in CO emission rates from peak values. Average 8-hour traffic rates are considerably lower than 1-hour peak volumes. Over the course of a typical day, meteorology and traffic commonly show bimodal patterns that are related to sunrise and sunset, and to morning and evening "rush hours". When high traffic volumes and low, steady winds occur simultaneously for an extended period of time, 8-hour CO levels are highest.

The extent to which traffic and meteorology change over time make it difficult to predict 8-hour CO levels using a Gaussian model such as CALINE4. Gaussian models assume that relatively steady-state, homogeneous conditions prevail. Fortunately, this is a reasonable assumption for worst case conditions.

One way of using CALINE4 to predict 8-hour average concentrations is to execute a multiple-hour run as described in the CALINE4 User Instructions(1). However, this approach requires hourly data for meteorology and traffic that are often difficult to determine.

The persistence factor can be used as an alternative to making a multiple-hour run in many modeling situations. Expressed as a ratio of the 8-hour to 1-hour second annual maximum CO concentration, it provides an easy way to

estimate an 8-hour CO maximum from a 1-hour value. One simply multiplies the predicted 1-hour second annual maximum by the persistence factor to obtain the corresponding 8-hour value. This factor offers a simple alternative to examining numerous combinations of hourly conditions.

The persistence factor was first recommended by the U. S. Environmental Protection Agency (EPA) in 1974(24). Initially, EPA recommended a persistence factor of approximately 0.6. Subsequent guidelines suggested values ranging from 0.6 to 0.7 and described a relationship in which higher persistence factors are associated with higher 1-hour CO concentrations(25,26). The 1978 CO Hot Spot Guidelines(27) concluded that 0.7 was a "...reasonable... standard value..." for cities where site-specific CO data were not available. It recommended values ranging from 0.7 to 0.8 where urban traffic was very heavy and stagnant air predominated throughout the day. Persistence factors of 0.6 to 0.7 were suggested for urban areas with better ventilation and where traffic was less congested.

Estimating 8-hour CO levels using a persistence factor has become popular since it was first recommended. This popularity is largely due to its ease of application. In addition, studies have shown that persistence factors occur within a fairly narrow range in a variety of geographic and urban settings(24,25,26,27). Conformity with EPA recommendations also helps make this an attractive option.

The purpose of the following analysis is to develop a method of computing a persistence factor that incorporates conditions at a project site. Evaluations of geography and land use influences also are discussed.

B. 8-Hour Persistence Factor

Two data sets were used to study persistence factors associated with differing land use and geography. The annual air quality summaries published by the California Air Resources Board (CARB) are one source of information(28). These summaries list maximum ambient CO levels at stations throughout the state. They were used to study the variability of persistence factors from site-to-site. The California Data Set (CDS), compiled during a previous Caltrans study(9), formed the second source of information. The stations in the CDS are also part of the CARB monitoring network, but the CDS spans a longer time period than the published annual summaries. Therefore, the CDS was more useful for studying variability of persistence factors from year-to-year.

The CDS consists of 1-hour and 8-hour seasonal maximums covering 112 station-years of data. These maximums were drawn from 12 stations with the average station-year composed of 329 days of 24 1-hour concentrations. Persistence factors were calculated for each season as the ratio of the 8-hour to 1-hour second highest CO concentration. Table 8-1 shows the sites and years represented in the CDS. The metropolitan population, used to indicate high or low urbanization, is also shown. An area/site code is used to identify each station in the Caltrans aerometric data bank.

Table 8-1. California Ambient CO Data Set (7).

Metro. Pop.	Location No.	Station	Area/Location Code	Years Studied	Total Seasons
	1	Pittsburg	700/430	1969-82	12
	2	Lancaster	7000/82	1971-82	10
<100k	3	Escondido	8000/115	1975-82	7
	4	Santa Barbara	4200/355	1974-82	7
	5	Salinas	2700/544	1976-82	5
	6	Bakersfield	1500/203	1972, 73, 76-79, 81, 82	5
100k to 500k	7	Stockton	3900/252	1965-67, 79-82	5
	8	Redwood City	4100/541	1968-82	13
	9	Sacramento	3400/582	1972-80	7
	10	Pomona	7000/75	1966-82	13
>500k	11	San Diego	8000/120	1973-82	8
	12	Burbank	7000/69	1963-82	19

The ranges of persistence factors shown in Figure 8-1 are in general agreement with previous findings(24,25,26,27). Persistence factors for less urban cities vary widely from 0.38 to 0.82. Factors in urbanized Pomona and Burbank range from 0.7 to 0.86. Lower factors in San Diego than in Burbank (both large urban sites) exemplify variability of persistence factors at some sites. The range of factors ,0.52 to 0.79, at this San Diego station (located in the downtown core at 1111 Island Avenue) also show that locally derived factors can differ dramatically from assumed values such as the commonly used 0.7 factor.

The means and standard deviations of the persistence factors at the CDS sites are shown in Table 8-2. The factors are plotted in Figures 8-2 to 8-4 for low (<100k), medium (100k-500k), and high (>500k) urbanization. The persistence factors at Burbank and Pomona are the highest and vary the least. Results for other stations in the CDS are not as consistent from year-to-year. There are several possible reasons for this difference. Travel patterns near the Burbank and Pomona monitoring stations have varied little over the past 20 years. Therefore, the ratio of 8-hour to 1-hour mobile emissions has remained fairly constant. Secondly, at heavily urbanized sites like Burbank and Pomona, the likelihood of stagnant meteorological conditions coinciding with uniformly high traffic emissions for both the 1-hour and 8-hour second-annual maximums is much higher than at less developed sites. This will cause the persistence factor to vary only slightly from one year to the next.

The Mann-Whitney statistic was used to measure significance of differences between persistence factors from the 12 CDS sites(20,21). The Burbank results were significantly higher than every other site except Pomona.

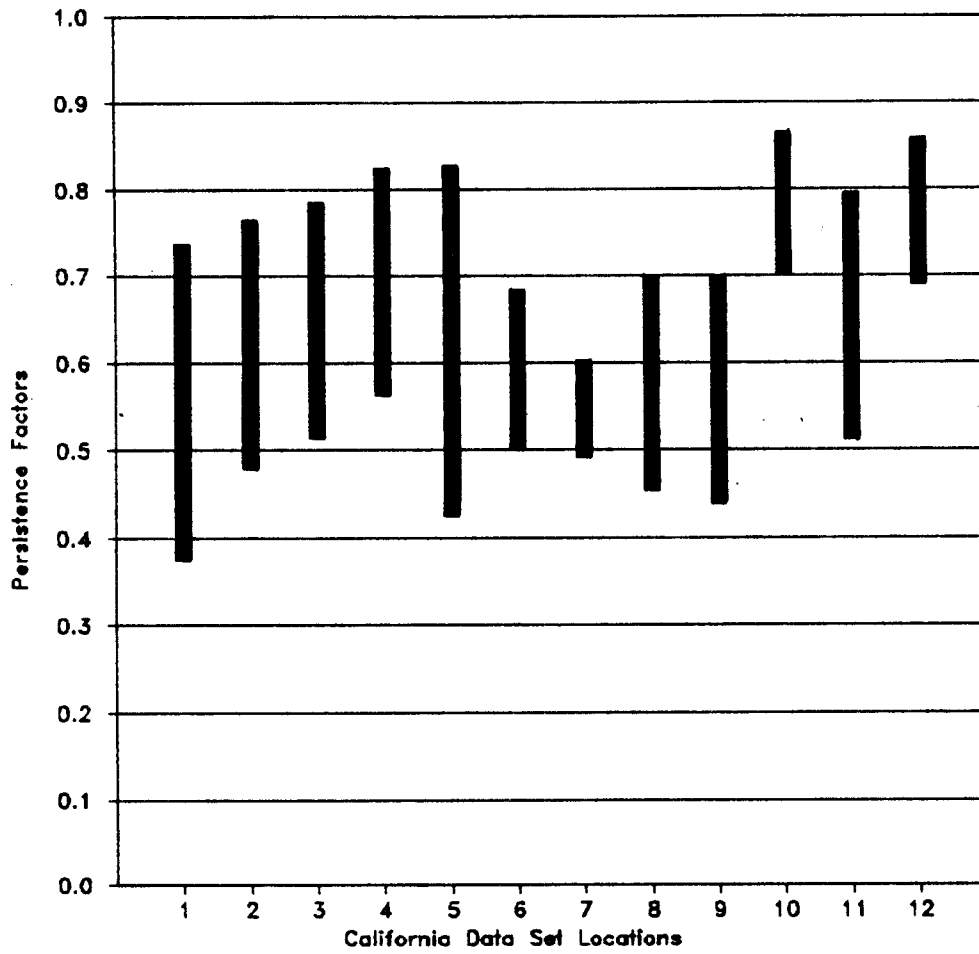


FIGURE 8-1. Ranges of Persistence Factors from CDS Sites.

Table 8-2. Statistical Characteristics of Persistence Factors in the California Data Set.

Station	Site No.	Mean	Standard Deviation	Maximum	Minimum
Pittsburg	1	.60	.09	.73	.38
Lancaster	2	.59	.08	.76	.49
Escondido	3	.62	.09	.78	.52
Santa Barbara	4	.67	.09	.82	.57
Salinas	5	.67	.14	.82	.43
Bakersfield	6	.60	.08	.68	.51
Stockton	7	.55	.04	.59	.50
Redwood City	8	.59	.08	.69	.46
Sacramento	9	.58	.09	.69	.45
Pomona	10	.78	.04	.86	.71
San Diego	11	.67	.11	.79	.52
Burbank	12	.79	.04	.85	.70

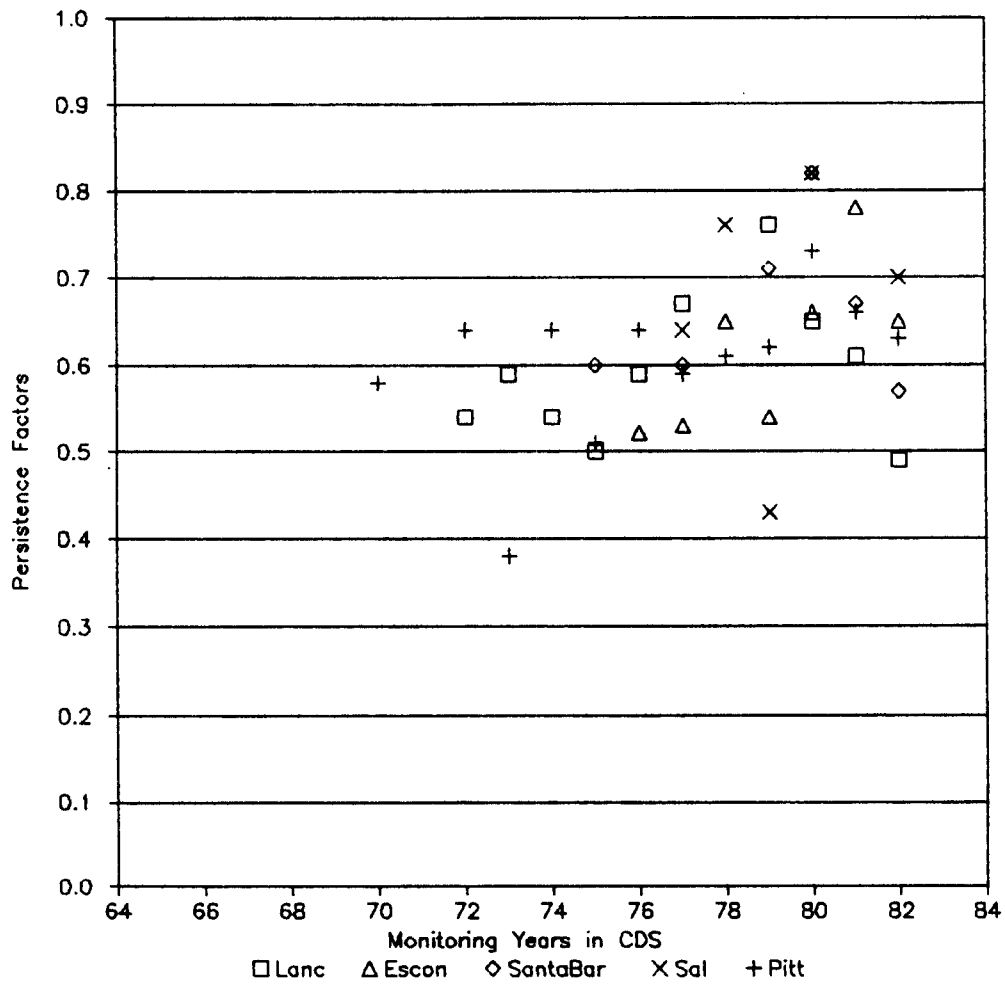


FIGURE 8-2. Persistence Factors at Less Populated (<100^k) CDS Locations.

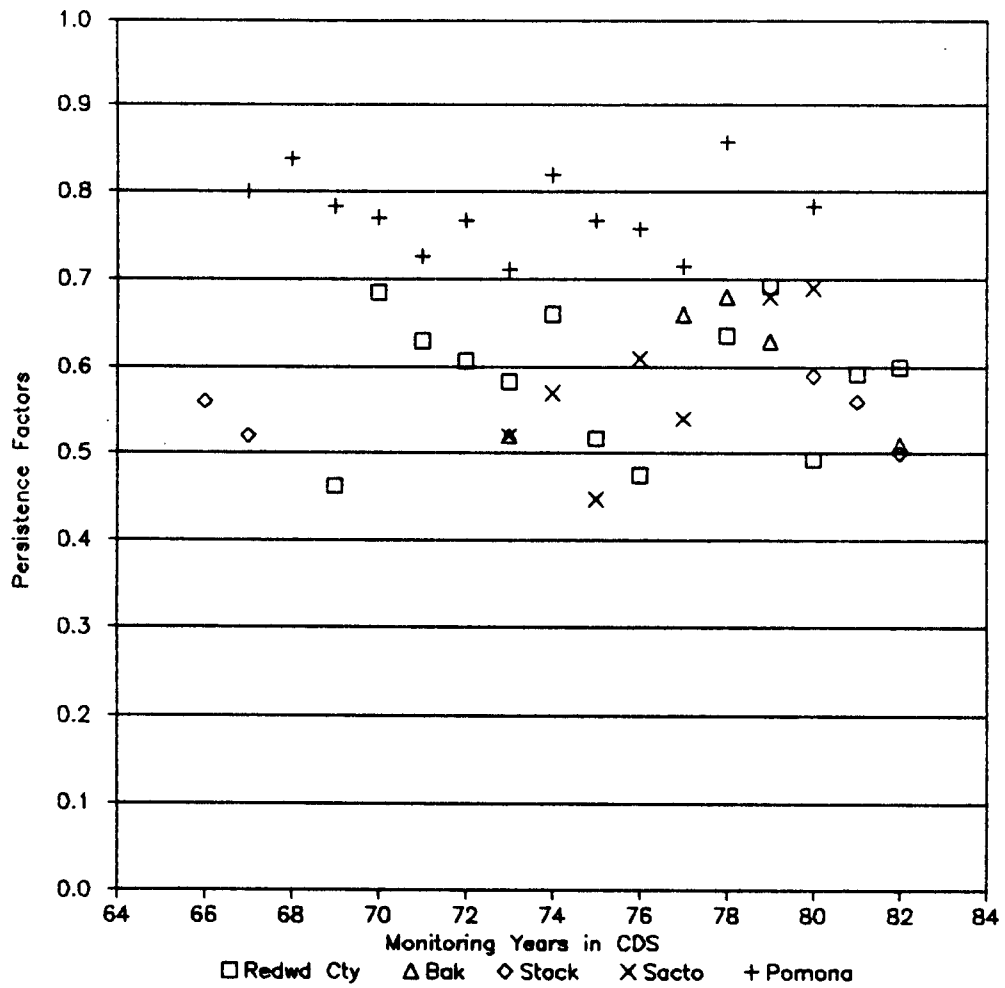


FIGURE 8-3. Persistence Factors at Medium Populated (100^k-500^k) CDS Locations.

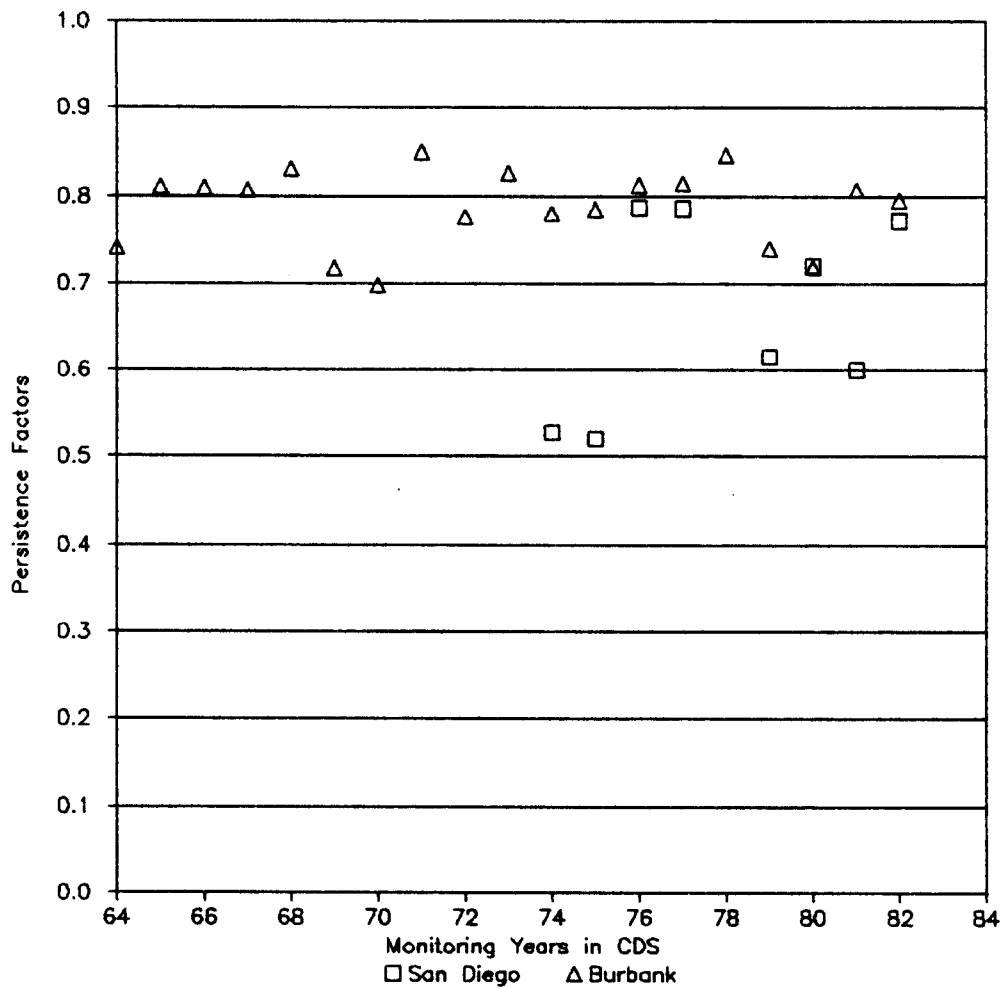


FIGURE 8-4. Persistence Factors at Densely Populated (>500^k) CDS Locations.

Pomona and Burbank were therefore grouped together as representing highly urbanized sites. San Diego data differed significantly from Burbank so it was removed from this evaluation. Persistence factors from the nine remaining sites were tested using the Kruskal-Wallis statistic(20,21). This test indicated that persistence factors from these sites were from the same general population. Therefore, they were grouped together as representing sites located in less urbanized (suburban and rural) communities. Cumulative frequency distributions in Figure 8-5 show substantially lower persistence factors in these less urban areas. The San Diego data were not included in Figure 8-5 since they are from a more urban site yet appear similar to data from less urbanized areas. The effects of varying traffic peak durations could not be tested directly because traffic counts near the CDS stations were not available. This was also a problem in studying the CARB summaries.

The CDS sites were grouped by geographic category (excluding Burbank and Pomona) to see if any systematic differences in persistence factors were apparent. The coastal sites of Santa Barbara and San Diego had the highest mean persistence factor of the groupings (0.67). The coastal valley sites of Escondido and Salinas followed at 0.65. Pittsburg and Redwood City, coastal valley sites near water, had a mean persistence factor of 0.60. Lowest of the groupings were the central valley sites (Stockton, Sacramento, Bakersfield and Lancaster), with a mean of 0.58. While these differences did not prove significantly different at the confidence level used for the statistical tests in this study (95%), they did form a recognizable pattern that may have some underlying basis.

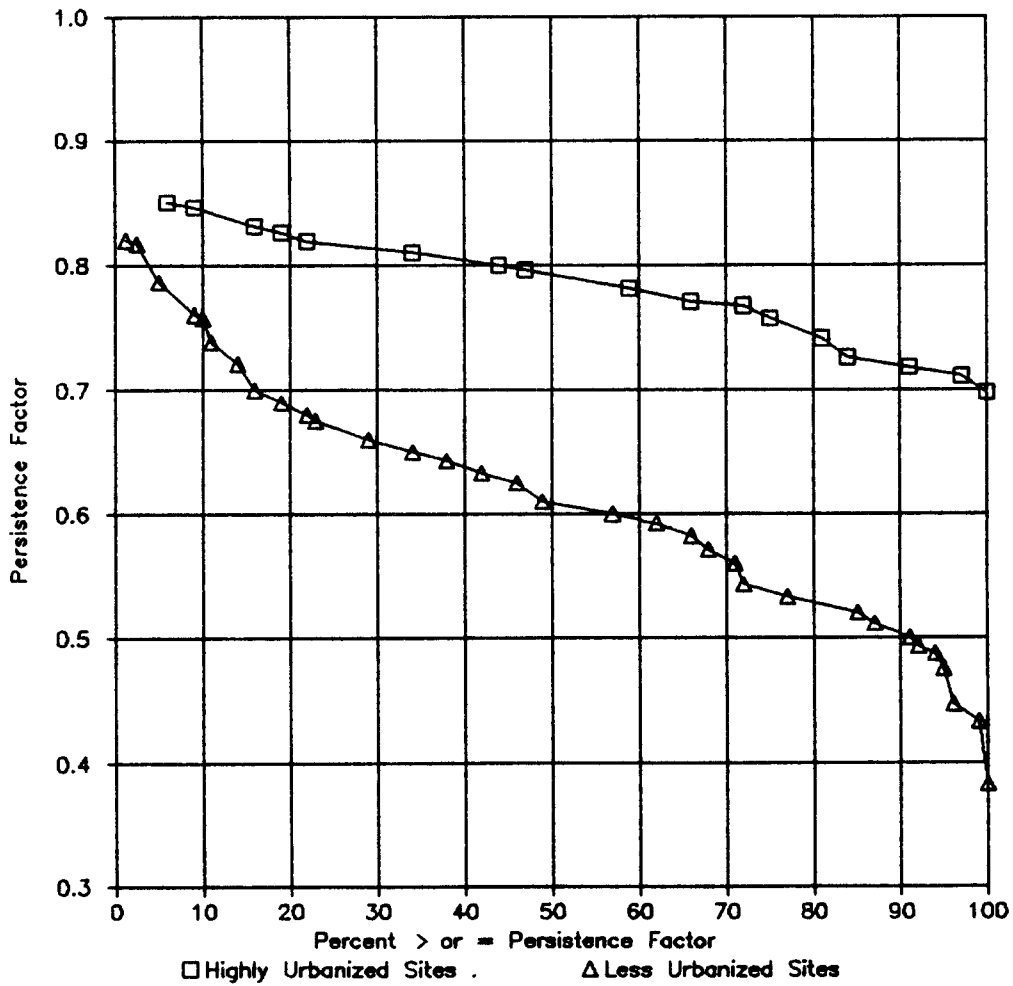


FIGURE 8-5. Cumulative Frequency Distributions of Persistence Factors (CDS).

The CARB summaries show first and second annual maximum CO levels at approximately 90 monitoring stations throughout California. These summaries were studied to further determine how urban and geographic settings influence the persistence factor. The summaries were also used to develop a method for determining site-specific persistence factors.

Persistence factors were computed at each site in the CARB monitoring network for calendar years 1981 to 1983. The CARB summaries categorize stations by air basin as shown in Table 8-3. Figure 8-6 shows ranges of persistence factors at all stations in each basin. Ranges of persistence factors were found to vary substantially between the basins. The South Coast Air Basin had higher average factors than in any other basin. Less scatter is apparent for South Coast stations for the same reasons mentioned earlier in connection with the Burbank and Pomona CDS results. For the other basins, persistence factors vary considerably.

Means, standards deviations, and ranges for all air basins are shown in Table 8-4.

As was seen in the CDS analysis, higher persistence factors are associated with heavily urbanized sites. Cumulative frequency plots in Figure 8-7 show substantially higher persistence factors in the heavily urbanized South Coast. Distribution of SCAB persistence factors appears in Figure 8-7(a) and (b) for easy comparison with coastal and inland basins. Basins with more than 3 station-years of measurements are shown in Figure 8-7.

Table 8-3. Number Of Stations In Each Air Basin
In the CARB Ambient CO Network.

Basin No.	Air Basin	Number of Stations
1	San Francisco Bay Area	17
2	North Central Coast	1
3	South Central Coast	2
4	South Coast	25
5	San Diego	8
6	Sacramento Valley	9
7	San Joaquin	12
8	Great Basin Valley	1
9	Southeast Desert	6
10	Mountain Counties	2
11	Lake County	1
12	Lake Tahoe	5

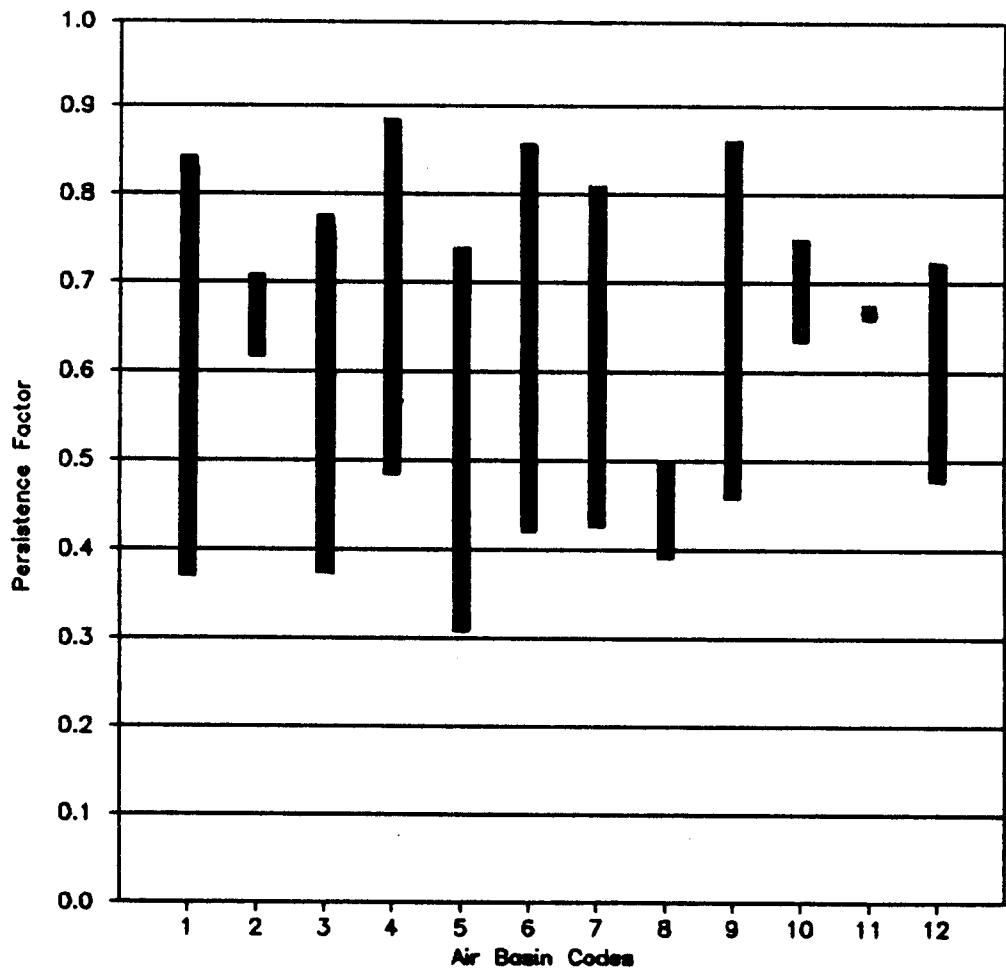


FIGURE 8-6. Ranges of Persistence Factors from CARB Summaries, 1981-83.

Table 8-4. Statistical Characteristics of Persistence Factors in Each Air Basin.

Air Basin	No. of Site-Yrs.	Mean	Standard Deviation	Max.	Min.
San Francisco Bay Area	48	.58	.11	.83	.38
North Central Coast	3	.68	.04	.70	.62
South Central Coast	15	.53	.12	.77	.38
South Coast	66	.70	.09	.85	.49
San Diego	21	.58	.11	.73	.32
Sacramento Valley	23	.60	.11	.82	.43
San Joaquin	33	.61	.12	.80	.44
Great Basin Valley	3	.45	.05	.49	.40
Southeast Desert	14	.60	.15	.85	.47
Mountain Counties	2	.70	.07	.74	.64
Lake County	1	.67	-	.68	.68
Lake Tahoe	15	.59	.07	.71	.49

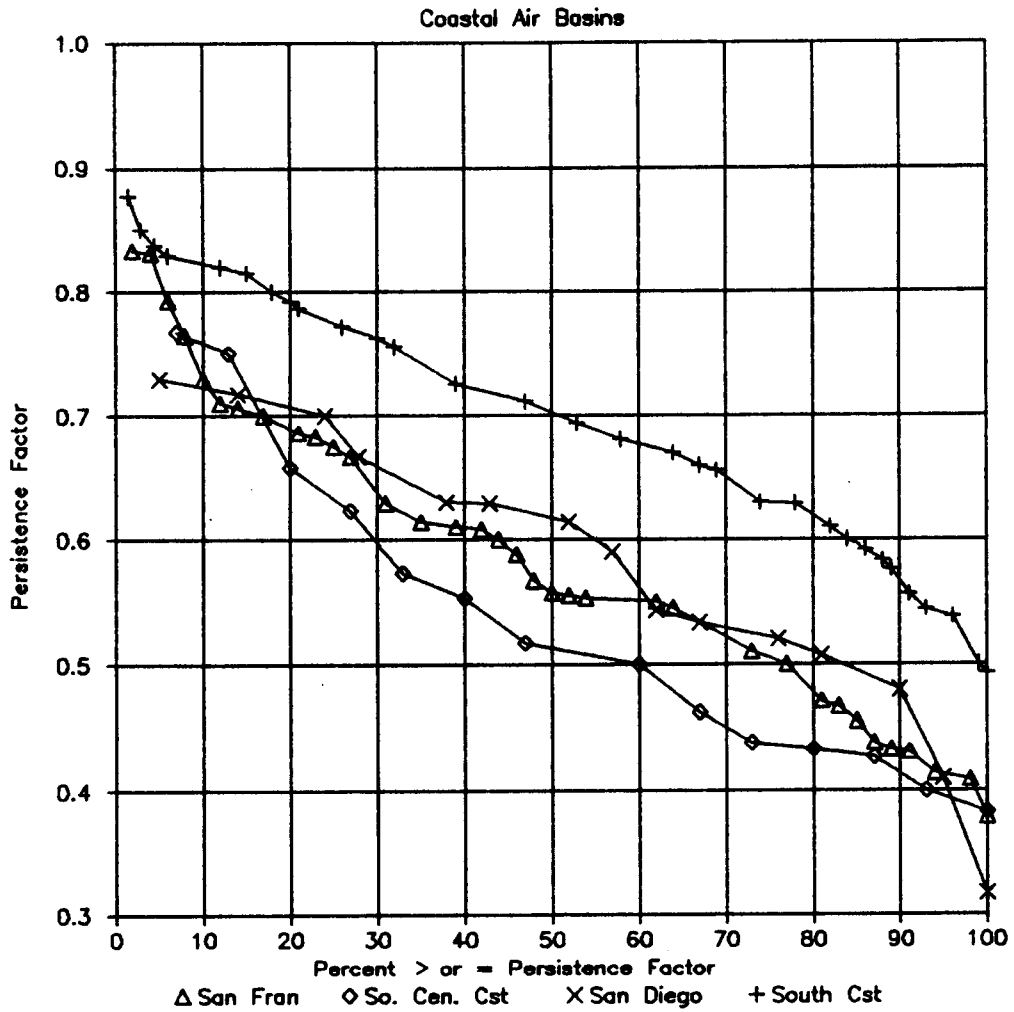


FIGURE 8-7(a). Cumulative Frequency Distributions of Persistence Factors in Coastal Basins (CARB data).

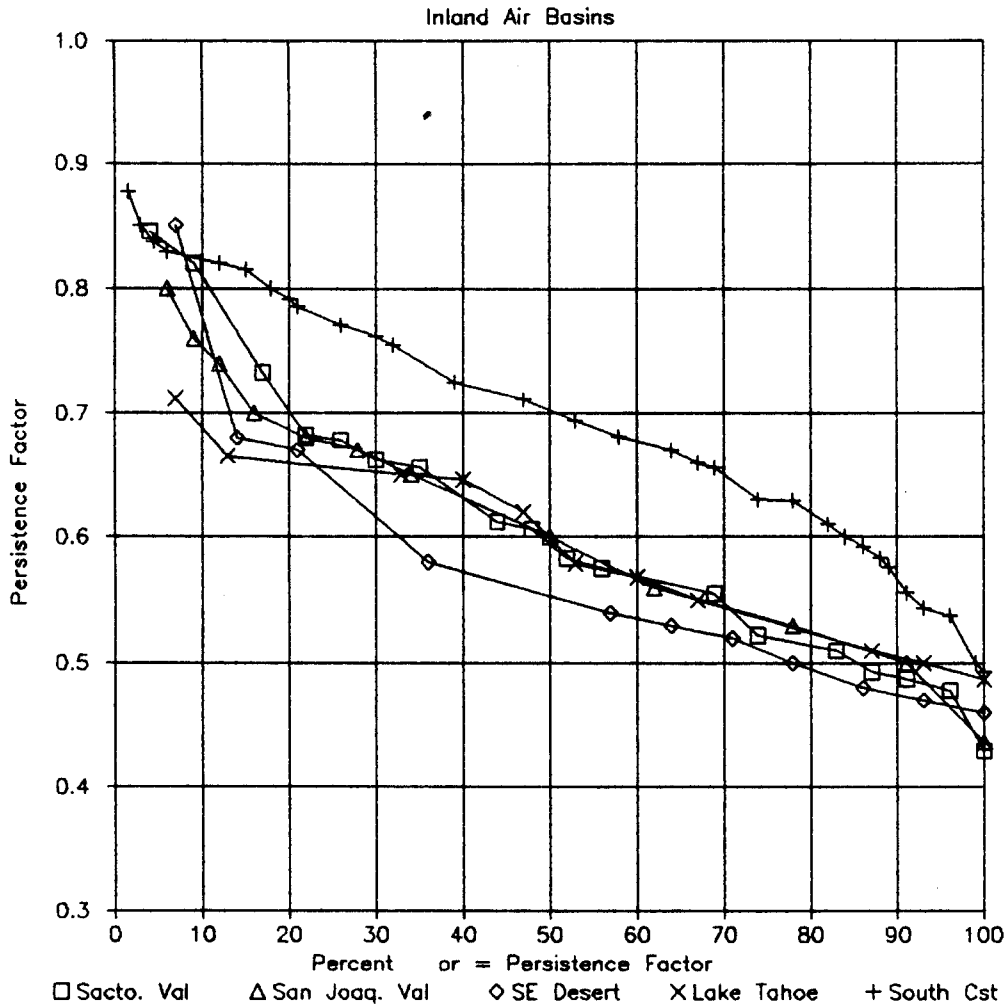


FIGURE 8-7(b). Cumulative Frequency Distributions of Persistence Factors in Inland Basins (CARB data).

Statistical techniques used previously on the CDS showed significant differences between urban and suburban sites for the CARB data also, reaffirming the CDS results. A significant difference was also found between urban sites in the South Coast and San Francisco Bay air basins. This was attributed to the less frequent occurrence of stagnant meteorological conditions in the San Francisco Bay Area. As was found in the CDS data, CARB data showed no significant differences that were attributable to geography alone, however.

In summary, analysis of the CDS and CARB data reveals that persistence factors for most sites are commonly below the recommended value of 0.7. Almost 85% of the persistence factors at the suburban CDS sites were below 0.7 with a mean value of 0.61, as shown in the cumulative frequency plot for CDS data shown in Figure 8-5. The predominance of factors less than 0.7 is typical in the CARB data as well.

Figure 8-7 shows only 15-25% of factors in all air basins except South Coast are higher than 0.7. Mean values are more in the range of 0.5 to 0.6.

The CDS and CARB data also show that persistence factors are considerably higher in developed urban centers. At urban CDS sites with potential for stagnant conditions, 97% of persistence factors were above 0.7, with a mean value of 0.78. In the South Coast the mean persistence factor is 0.7 with nearly 85% of factors higher than 0.6.

These results suggest that locally derived persistence factors are more appropriate to use when available than the default values recommended by EPA. The accuracy of

8-hour CO estimates should improve when the persistence factor is based on CO levels at a site with land use and geographic characteristics similar to the proposed project location. The CO maximums summarized for the many air quality monitoring stations located in California and other states are ideal for this purpose.

The CARB and CDS data sets were examined to develop a method for calculating locally derived persistence factors. The CARB summaries represented three years of data (1981 to 1983). These results were compared to the long-term data for the 12 CDS stations. The maximum persistence factors for the three year period correlated well to the corresponding long-term, average CDS values (Table 8-5 and Figure 8-8). The relative error between the two was typically less than 5%.

Based on these results, it is recommended that the maximum ratio of the 8-hour to 1-hour second annual maximum CO concentration over the most recent three year period at a nearby, representative continuous air monitoring station be used as the persistence factor to estimate 8-hour worst case CO concentrations from 1-hour levels. If no nearby, representative data are available, a persistence factor of 0.6 should be used for rural and suburban locations, and 0.7 for urban locations. If the urban site is located in an area with a recognized tendency for persistent stagnant meteorological conditions, a factor of 0.8 should be used.

C. 8-Hour Worst Case Meteorology

Circumstances may arise during the course of an air quality impact analysis that preclude the use of a persistence factor. The best example of this is a situation in which two project alternatives with traffic

Table 8-5. Comparison of CDS Mean and CARB
3-Year Maximum Persistence Factors.

SITE	NO. OF YEARS IN CDS	MEAN OF CDS PERIOD	3 YEAR CARB MAX.	RELATIVE ERROR
Burbank	19	.79	.82	1.9%
Pomona	13	.78	.79	0.6%
Redwood City	13	.59	.63	3.3%
Pittsburg	12	.60	.63	2.4%
Lancaster	10	.59	.54	-4.4%
San Diego	8	.67	.72	3.6%
Escondido	7	.62	.67	3.9%
Santa Barbara	7	.67	.62	-3.9%
Stockton	5	.55	.57	1.8%
Salinas	5	.67	.70	2.2%
Bakersfield	5	.60	.62	1.6%

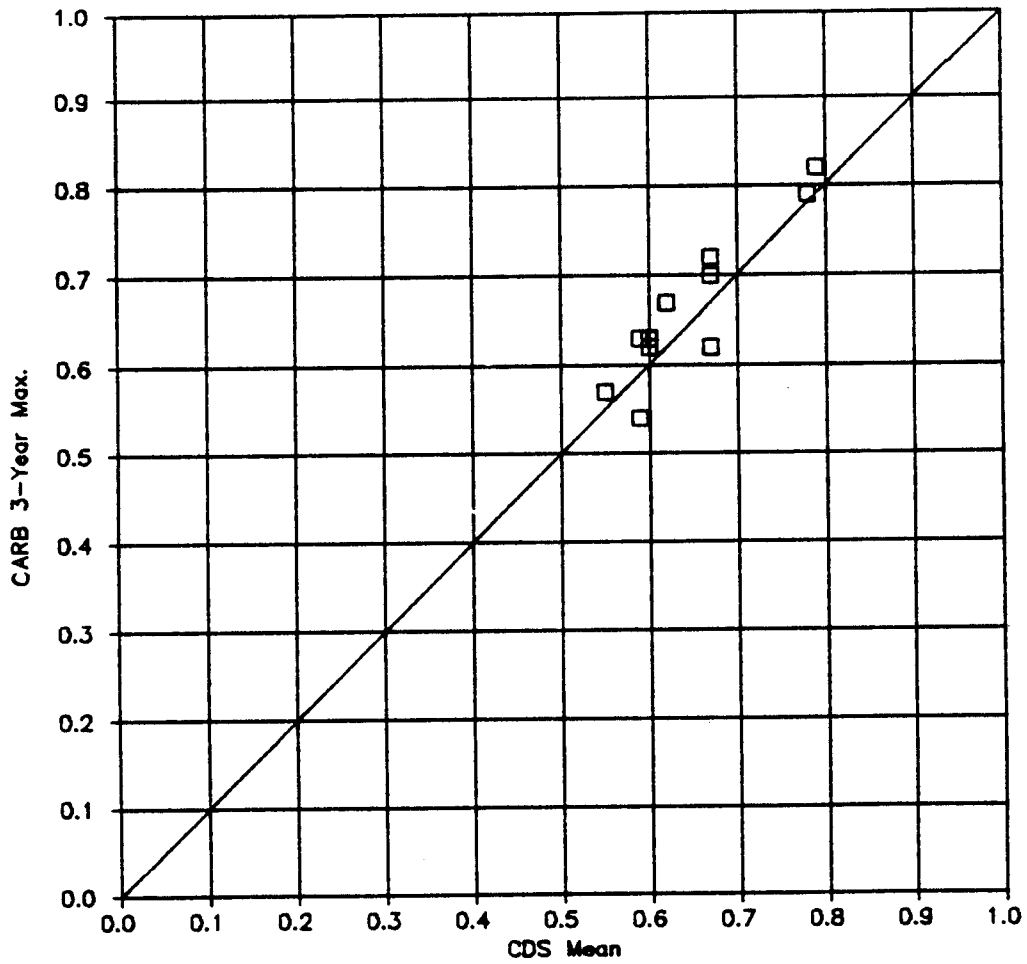


FIGURE 8-8. Maximum Persistence Factors from 1981-83 Versus Means from CDS.

peaks of similar magnitude but different duration must be compared. Since the peak volumes and emission factors are similar, the predicted 1-hour worst case CO concentrations are likely to be close. Applying the same persistence factor to both 1-hour values will yield correspondingly close 8-hour levels. Yet, the project with the longer traffic peak should yield a higher 8-hour worst case concentration. An analysis that uses the persistence factor does not address this difference.

In order to handle this kind of problem effectively, a set of recommended worst case 8-hour meteorological scenarios were developed from the same data base used for the 1-hour recommendations. The data base was not analyzed in the same rigorous, probabilistic fashion, however. Instead, the data were screened, using a specific selection criteria, and the resulting worst case 8-hour episodes summarized and studied.

As with the 1-hour analysis, time-of-day periods were defined for the purposes of matching the 8-hour meteorological episodes with typical traffic patterns. Three overlapping periods were studied: morning (0600-1400), midday (1000-1800) and evening (1400-2200). Within each of these 8-hour periods the hourly data were further categorized according to expected traffic conditions, either peak or off-peak. The assumed three hour peak conditions were defined as follows: morning (0600-0900), midday and evening (1500-1800).

For both peak and off-peak conditions, average measures for wind speed and sigma theta were determined. Average wind speed was calculated by averaging the reciprocal of the hourly values. Since wind speed is inversely proportional to concentration in the conventional Gaussian

equation, this was equivalent to averaging a series of hourly concentrations. Consequently, these values could be used to study the combined effect on an average concentration of consecutive hours with varying wind speeds. The hourly sigma theta results were averaged in the conventional root-mean-square manner. That is, they were converted to variances by squaring, averaged, and finally reconverted by taking the square root of the averaged value.

The daily 8-hour results for each site/time period combination were ranked by consistency of wind direction. The reason for organizing the data in this fashion was to eliminate from consideration the numerous 8-hour periods during which major shifts in wind direction occurred. Such periods are not consistent with worst case conditions or Gaussian methodology. The standard deviation of the average hourly wind direction was used as the measure of wind direction consistency(29).

The resulting ranked data were screened for worst case 8-hour scenarios. A weighted value for the MSI based on average wind speed and sigma theta for peak and off-peak conditions was used to help select the scenarios. Two cases were chosen: one for periods with wind direction consistency measures less than or equal to 15° , and a second for periods with consistency measures less than or equal to 45° . The 15° limitation represented conditions consistent with winds parallel to a highway alignment. The 45° limitation was consistent with perpendicular winds (crosswind case). Depending on the geometry of a particular problem, one of these two cases will likely be the worst case.

The selected cases were summarized by site and time-of-day period (Tables 8-6 and 8-7). These results were studied for systematic differences between site, time period, and wind orientation. There were clear differences throughout the data between the peak and off-peak time periods and the parallel and crosswind cases. Site-to-site differences were much less consistent. A set of recommended worst case 8-hour scenarios was developed from these results and is given in Tables 8-8 and 8-9. The values for stability class are consistent with the corresponding wind speed and time period. Recommended temperature adjustments are consistent with the 1-hour methodology.

In cases where use of a persistence factor is inappropriate for determining 8-hour air quality levels and when insufficient data are available for multiple-hour model runs, the meteorological inputs recommended in Tables 8-8 and 8-9 can be used.

Table 8-6. Crosswind Case (Sigma Theta \leq 45 degrees)
Peak & Off-Peak Monitoring Data Summaries.

Time Period	Site	PEAK (3 Hours)		OFF-PEAK (5 Hours)	
		Wind Speed	Sigma Theta	Wind Speed	Sigma Theta
Morning 0600- 1400	Gilroy	0.7	67	1.6	41
	San Jose	0.5	59	1.3	39
	Half Moon	0.8	69	1.3	26
	Mammoth	0.7	33	2.0	23
	Convair	0.4	30	1.5	27
	Santee	0.3	36	0.6	46
	Lab	0.2	24	0.4	26
	CHP	0.2	29	1.0	80
Bksfld.	1.2	26	2.7	28	
Midday 1000- 1800	Gilroy	1.5	17	1.3	49
	San Jose	0.9	19	1.1	51
	Half Moon	1.0	55	1.3	42
	Mammoth	0.6	78	1.2	23
	Convair	0.6	13	1.4	29
	Santee	0.8	18	0.8	14
	Lab	0.4	24	0.3	26
	CHP	0.3	28	1.5	34
Bksfld.	2.0	21	1.7	57	
Evening 1400- 2200	Gilroy	2.1	17	0.8	46
	San Jose	0.5	45	0.5	39
	Half Moon	1.2	41	1.2	42
	Mammoth	0.9	17	0.5	16
	Convair	1.2	18	0.4	37
	Santee	0.6	84	0.5	25
	Lab	0.4	24	0.4	24
	CHP	0.7	17	0.5	28
Bksfld.	2.3	25	1.4	46	

Note: Sigma theta values were estimated at Convair, Santee, Lab, CHP, and Bakersfield(4,5).
Wind speed is in m/s and sigma theta in degrees.

Table 8-7. Parallel Case (Sigma Theta \leq 15 degrees)
Peak & Off-Peak Monitoring Data Summaries.

Time Period	Site	PEAK (3 Hours)		OFF-PEAK (5 Hours)	
		Wind Speed	Sigma Theta	Wind Speed	Sigma Theta
Morning 0600- 1400	Gilroy	1.4	20	1.8	19
	San Jose	2.8	15	2.7	17
	Half Moon	2.0	19	2.2	25
	Mammoth	2.6	32	3.4	29
	Convair	0.5	18	2.3	15
	Santee	-	-	-	-
	Lab	0.6	21	1.0	24
	CHP	1.6	16	1.8	38
	Bksfld.	2.0	21	2.8	30
Midday 1000- 1800	Gilroy	1.7	10	2.3	17
	San Jose	0.9	19	1.9	20
	Half Moon	1.9	21	3.1	16
	Mammoth	0.9	17	1.2	23
	Convair	1.1	17	1.9	20
	Santee	1.4	12	1.0	51
	Lab	1.0	23	1.2	24
	CHP	0.7	21	2.1	32
	Bksfld.	2.6	20	1.9	43
Evening 1400- 2200	Gilroy	2.7	9	1.8	22
	San Jose	1.2	13	1.0	14
	Half Moon	2.6	15	2.3	14
	Mammoth	0.9	17	0.5	16
	Convair	1.3	27	0.8	15
	Santee	0.8	18	0.7	10
	Lab	0.8	16	0.4	24
	CHP	3.0	9	3.2	10
	Bksfld.	4.6	16	2.9	16

Note: Sigma theta values were estimated at Convair, Santee, Lab, CHP, and Bakersfield(4,5).
Wind speed is in m/s and sigma theta in degrees.

Table 8-8. Crosswind Case -- Suggested Worst Case
8-Hour Meteorological Scenarios.

Geographic Location	PEAK				OFF-PEAK			
	Wind Speed	Sigma Theta	Stab. Class	Temp.	Wind Speed	Sigma Theta	Stab. Class	Δ Temp.
MORNING								
Coastal	0.5	45	"G"	+5	1.5	30	"D"	+10
Coastal Val.	0.5	45	"G"	+5	1.0	45	"D"	+10
Central Val.	0.5	45	"G"	+5	0.5	45	"D"	+10
Mountain	0.5	45	"G"	+5	1.5	30	"D"	+10
MIDDAY								
Coastal	0.5	45	"G"	+5	1.5	30	"D"	+10
Coastal Val.	0.5	45	"G"	+5	1.0	45	"D"	+10
Central Val.	0.5	45	"G"	+5	0.5	45	"D"	+10
Mountain	0.5	45	"G"	+5	1.5	30	"D"	+10
EVENING								
Coastal	0.5	45	"G"	+5	0.5	45	"D"	+5
Coastal Val.	0.5	45	"G"	+5	0.5	45	"D"	+5
Central Val.	0.5	45	"G"	+5	0.5	45	"D"	+5
Mountain	0.5	45	"G"	+5	0.5	45	"D"	+5

Note: Wind speed is in m/s, sigma theta in degrees, and Δ temperature in degrees Fahrenheit.
Add Δ temperature to lowest January mean minimum temperature over three year period.

Table 8-9. Parallel Case -- Suggested Worst Case
8-Hour Meteorological Scenarios.

Geographic Location	PEAK				OFF-PEAK			
	Wind Speed	Sigma Theta	Stab. Class	Temp.	Wind Speed	Sigma Theta	Stab. Class	Δ Temp.
MORNING								
Coastal	1.0	20	"G"	+5	2.0	20	"D"	+10
Coastal Val.	1.0	20	"G"	+5	2.0	20	"D"	+10
Central Val.	0.5	20	"G"	+5	1.0	20	"D"	+10
Mountain	1.0	20	"G"	+5	2.0	20	"D"	+10
MIDDAY								
Coastal	1.0	20	"G"	+5	2.0	30	"D"	+10
Coastal Val.	1.0	20	"G"	+5	2.0	45	"D"	+10
Central Val.	1.0	20	"G"	+5	1.0	45	"D"	+10
Mountain	1.0	20	"G"	+5	2.0	30	"D"	+10
EVENING								
Coastal	1.0	20	"G"	+5	1.0	20	"G"	+5
Coastal Val.	1.0	20	"G"	+5	1.0	20	"G"	+5
Central Val.	1.0	20	"G"	+5	1.0	20	"G"	+5
Mountain	1.0	20	"G"	+5	1.0	20	"G"	+5

Note: Wind speed is in m/s, sigma theta in degrees, and Δ temperature in degrees Fahrenheit.
Add Δ temperature to lowest January mean minimum temperature over three year period.

REFERENCES

1. P. E. Benson, CALINE4 - A Dispersion Model For Predicting Air Pollution Concentrations Near Roadways, Caltrans, FHWA/CA/TL-84/15, November 1984.
2. P. E. Benson, CALINE3 - A Versatile Dispersion Model for Predicting Air Pollutant Levels Near Highways and Arterial Streets, Caltrans, FHWA/CA/TL-79/23, November 1979.
3. S. Kassel and W. Winter, Automated Methods of Acquiring and Reducing Aerometric Data, Caltrans, CA/DOT/TL-7157-1-76-08, March 1976.
4. E. H. Markee, On the Relationship of Range to Standard Deviation of Wind Flucuation, Monthly Weather Review, pp 83-87, February 1963.
5. K. A. Verral and R. L. Williams, A Method for Estimating the Standard Deviation of Wind Directions, Journal of Applied Meteorology, V. 21, pp 1922-1925, 1982.
6. D. Golder, Relations Among Stability Parameters in the Surface Layer, Boundary-Layer Meteorology, V. 3, pp 47-58, 1972.
7. D. Coats, R. Bushey, and E. Shirley, Mobile Source Emission Factors, Caltrans, CA/TL-80/15, May 1980.
8. K. Brodtman and T. Fuca, Determination of Hot and Cold Starts Percentages in New Jersey, Final Report, New Jersey Department of Transportation, Bureau of Transportation Technology Research, HPR Study No. 7792, June 1982.
9. P. E. Benson, Measurement and Analysis of Ambient Carbon Monoxide Concentrations for Project-Level Air Quality Impact Studies, Caltrans, FHWA/CA/TL-84/01, February 1984.
10. J. Horowitz and S. Barakat, Statistical Analysis of the Maximum Concentration of an Air Pollutant: Effects of Autocorrelation and Non-Stationarity, Atmospheric Environment, V. 13, pp 811-818, 1979.
11. S. R. Hanna, Lateral Turbulence Intensity and Plume Meandering During Stable Conditions, Journal of Climate and Applied Meteorology, V. 22, pp 1424-1430, August 1983.
12. W. S. Meisel and T. E. Dushane, Monitoring Carbon Monoxide Concentrations in Urban Areas, TRB, NCHRP 200, April 1979.

13. M. Liu and G. Moore, On the Evaluation of Predictions from a Gaussian Plume Model, Journal of the Air Pollution Control Association, V. 34, No. 10, pp 1044-1050, October 1984.
14. J. B. Kennedy and A. M. Neville, Basic Statistical Methods for Engineers and Scientists, Harper & Row, 1976.
15. M. J. Hinich and K. D. Mackenzie, Introduction to Continuous Probability Theory, Merill Publishing Co.
16. C. Derman, L. Gleser, and I. Olkin, A Guide to Probability Theory and Application.
17. R. A. Gangolli and D. Ylvisaker, Discrete Probability, Harcourt, Brace, Jovanovich.
18. D. Mackay and S. Paterson, Spatial Concentrations Distributions, Environmental Science and Technology, V. 18, No. 7, pp 207A-214A, 1984.
19. M. Abramowitz and I. Stegun, editors, Handbook of Mathematical Functions, Dover Publications, Inc.
20. S. Siegel, Non-Parametric Statistics: For the Behavioral Sciences, McGraw-Hill Book Co., 1956.
21. J. V. Bradley, Distribution-Free Statistical Tests, Prentice-Hall Inc., 1968.
22. G. Long, Meteorological Conditions for Predicting Air Quality Near Highways in Florida, Transportation Research Center, University of Florida, February 1984.
23. National Oceanic and Atmospheric Administration, Climatological Data, California (1979-1983), National Weather Service, V. 85-89.
24. R. Patterson et.al., Validation Study of An Approach for Evaluating the Impact of A Shopping Center On Ambient Carbon Monoxide Concentrations, GCA Corporation, EPA Contract No. 68-02-1376, August 1974.
25. Guidelines for Air Quality Maintenance Planning and Analysis Volume 9: Evaluating Indirect Sources, Environmental Protection Agency, EPA-450/4-75-001, January 1975.
26. Guidelines for Air Quality Maintenance Planning and Analysis Volume 9 (Revised): Evaluating Indirect Sources, Environmental Protection Agency, EPA-450/4-78-001), September 1978.

27. F. Benesh, Carbon Monoxide Hot Spot Guidelines, Volume II: Rationale, GCA Corporation, Environmental Protection Agency, Contract No. 68-02-2539, August 1978.

28. California Air Quality Data, Annual Summary of Air Quality Data, 1981-1983, California Air Resources Board, V. XIII-XV.

29. R. J. Yamartino, A Comparison of Several "Single-Pass" Estimators of the Standard Deviation of Wind Direction, Journal of Climate and Applied Meteorology, V. 23, pp 1362-1366, September 1984.